Chapter 5. Microstructures

5.1 Introduction

Microstructures earlier designated as "Texture" (Barkar, 1998) are the micro-scale features used in decoding the tectonic and metamorphic history of rocks. These microstructures synchronous with the deformation mechanisms, can be classified as, (i) Micro-fractures, rigid particle displacement and rotation due to the process of cataclasis; (ii) Material removal, transport and deposition on account of diffusive mass transfer by solution; (iii) Permanent distortion of the crystal lattice by the virtue of intracrystalline plasticity (Blenkinsop, 2000). The present chapter deals with the identification and categorization of the microstructures developed within representative rocks by correlating it with the regional deformation and thermal event.

As mentioned in chapter 3, the Champaner region comprises varieties of rock types such as quartzites, meta-greywackes, meta-conglomerates, schists, phyllites, slates, hornfelses and granites. However, rocks that have preserved microstructural features like preferred orientation of new minerals, as also recrystallization microstructures in response to the deformational and metamorphic events have been picked up for the said analyses. In order to elucidate the derivatives of each event, the microstructures have been categorized as (i) Temperature and/or Strain Induced Microstructures (TSIMs) (ii) Shear Induced Microstructures (SIMs) (iii) Complex Microstructures (CMs). In later part of this chapter, an attempt has been made to correlate these microstructures with the regional scale folding and shearing as well as with the emplacement of the thermal event. A time relationship vis-à-vis the crystallization and deformation has been established by summarizing all events witnessed by rocks in the study area within the Champaner region.

---

* The part of this chapter is based on our paper published:
(a) Patel, D, Joshi, A U, Limaye, M A (2016) Sequential development of microstructures in Quartzites of Champaner Group, Gujarat: An Implication of Godhra Granite. Journal of Geosciences Research, vol. 1 No. 2, pp. 101-104.

5.2 Temperature and/or Strain Induced Microstructures (TSIMs)

Naturally deformed rocks reveal crystals with defects such as point, line or plane (Hobbs et al., 1976). The density of these defects increases due to the deformation of a crystal caused at relatively low temperatures and/or rapid strain rates (Hobbs et al., 1976; Spry, 1969; Vernon, 1976; Nicholas and Poirier, 1976). The phenomenon called as “Work-hardening” (similar to that of cold-working in metals) suggests, increase in dislocation density leading to crystal hardening and requires more amount of stress to deform it further (Ghosh, 1985; Dieter, 1988). In case of such crystals there exists higher internal energy and are thermodynamically less stable (Mamtani and Karanth, 1996b). If an external heat source is provided, the instability of a deformed crystal increases rapidly causing grain softening and reverting of the crystal back in the strain free condition by the virtue of grain growth or “Annealing” (Ghosh, 1985; Dieter, 1988). Due to the sub-processes of annealing, referred to as “Recovery and Recrystallization”, the deformed grain attains thermodynamic stability and results into coarsening of grains. The present section explains the TSIMs developed within quartzites of the Champaner Group due to the deformation and effect of heat as well as the strain imparted by the Godhra granitic intrusion.

Petrographic study of quartzites from different localities, which are away from the granite reveals granoblastic polygonal, mosaic with two granular boundary varieties (i.e.) Inequigranular Interlobate and Seriate Interlobate (Fig. 5.1a, b). The former type is observed in the quartz grains showing sutured boundaries with large scale variability in grain size, whereas the latter shows less size variation with sutured grain boundaries. These boundaries are on account of high strain along with moderate temperature prevailing over quartzites and empowering effect of dynamic recrystallization. The grains show inclusions of mica flakes especially muscovite having colourless to faint green pleochroism.

a. b.

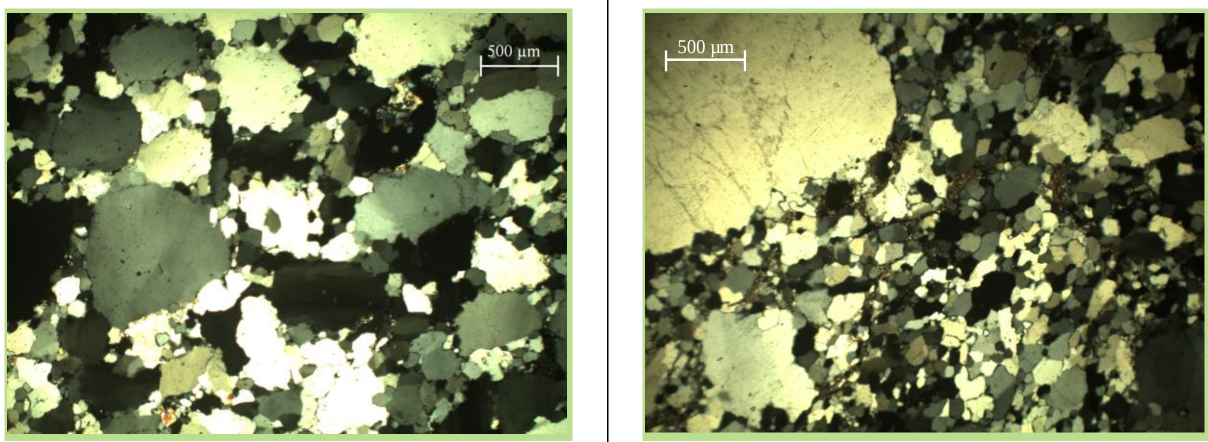

Figure 5.1: Photomicrograph of quartzite showing: (a) Granoblastic polygonal texture with inequigranular interlobate boundary and (b) Granoblastic polygonal texture with seriate interlobate boundary.

At places, the phenomena of Grain Boundary Migration (GBM) and Grain boundary Bulging (BLG) with sweeping undulose extinction are also observed. Some quartz grains show strain free appearance due to phenomenon of rapid recrystallization and recovery. The sub-grain rotation (SGR) phenomenon is also observed, which is reflected by progressive disorientation of sub-grains compared to surrounding older grains.

The quartz grains in the quartzites nearer to granite show interlocking with straight grain boundaries meeting at triple junction, having sharp extinction. The presence of 120° triple points, referred to as foam microstructure by Vernon (1976), is indicative of heat outlasting deformation or annealing. These microstructural characteristics clearly point to static recrystallization with Grain Boundary Area Reduction (GBAR) as the principal mechanism.

5.2.1 Bulging Recrystallization (BLG)

Bulging (BLG) recrystallization occurs at low temperature in which the boundary of one grain bulges into the adjacent grain, having high dislocation density (Fig. 5.2 a). The resultant feature forms a new grain at the periphery of the older one (Baily and Hirsch, 1962; Drury et al., 1985; Shigematsu, 1999; Stipp et al., 2002). Quartzites located in and around Bamankuwa, Dolimaar and south of Dolimaar are characterized by bulging recrystallization or low temperature grain boundary migration that belongs to regime 1 of (Hirth and Tullis, 1992). It can be seen that grain boundary of one grain of quartz is bulging into the other due to difference in dislocation density (Fig. 5.2b). This has formed along the boundaries of the relict grains resulting in uneven grain shape and size. Such bulging is typically seen in strongly deformed quartz having temperature less than 300°C (Wu and Groshong, 1991a).

a.

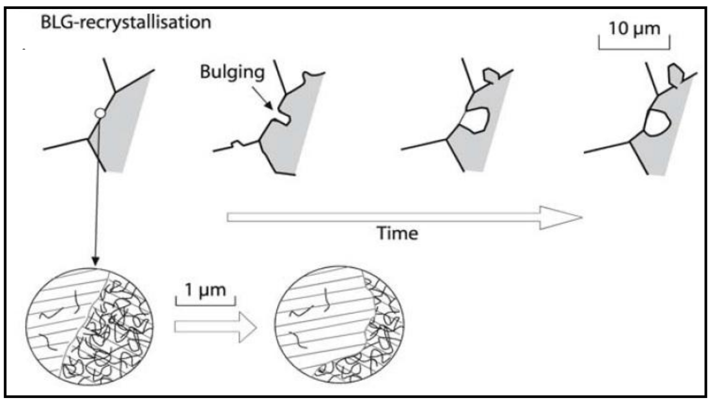

b.

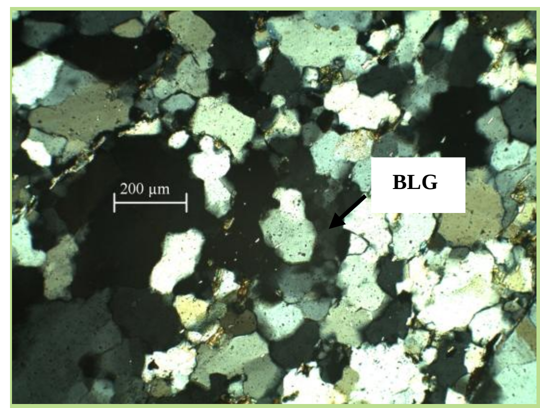

Figure 5.2: (a) Schematic sketch showing stages of Bulging recrystallization (BLG), the grain with higher dislocation density (shaded) is consumed by bulging of less deformed grain. Finally, the bulged grain developed as individual grain. Figure 5.2a is after Passchier and Trouw, 2005; P.42. (b) Photomicrograph of quartzite of study area showing BLG recrystallization. The grain boundary of one grain of quartz is bulging into the other.

5.2.2 Subgrain Rotation Recrystallization (SGR)

The process of subgrain rotation recrystallization results into a new grain formation that has high angle offset relation with the neighboring grains (Fig. 5.3a). It has been found in quartzites of Keshavpura area and up to Malabar in south of the study area. Such special recrystallization is due to adding up of dislocations to subgrain boundaries of newly formed grain. In present case, the quartz grain shows disorientation with respect to surrounding host grains (Fig. 5.3b) and generally occurs at crystallization temperature more than 300°C. A new grain is developed with a transition from low angle to high angle in relation to relict old grains. This SGR microstructure corresponds to regime 2 of (Hirth and Tullis, 1992).

a.

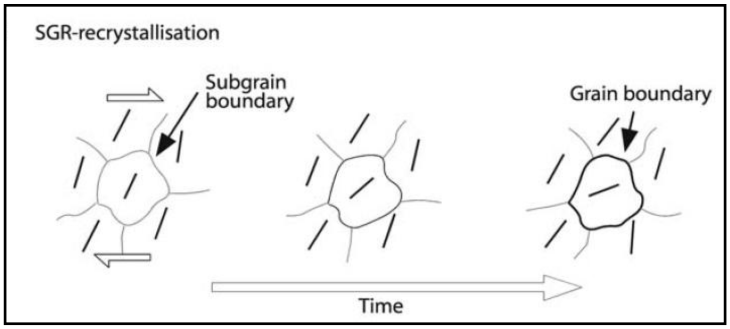

b.

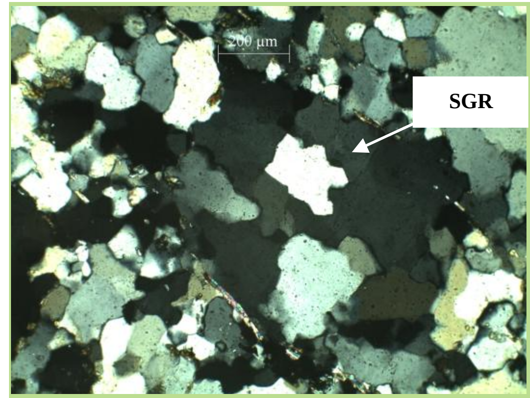

Figure 5.3: (a) Schematic sketch showing stages of Sub-grain rotation recrystallization (SGR), which results into a new grain formation that has high angle offset relation with the neighboring grains. Bars in the subgrains indicate lattice orientation. Figure 5.3a is after Passchier and Trouw, 2005; P.42. (b) Photomicrograph of quartzite of the study area showing SGR recrystallization. Quartz grain shows disorientation with respect to surrounding host grains.

5.2.3 Grain Boundary Migration Recrystallization (GBM)

The quartzites found near Lambhia and Mota Raska village demarcate presence of GBM which occurs at comparatively higher temperature condition than SGR. In these types of microstructures, grain boundaries become mobile and sweep throughout the grain to remove dislocations (Fig. 5.4a). Due to GBM, all dislocations are found to be removed from quartz grains, resulting in inequigranular interlobate boundaries. In case of the quartzites referred to above, the variability in grain size makes it difficult to distinguish between new and older grains (Fig. 5.4b). The left over grains show grain boundary migration recrystallization and correspond to regime 3 of (Hirth and Tullis, 1992). Due to such recrystallization process, the quartz grains are strain free and show straight extinction (Passchier & Trouw, 2005).

a.

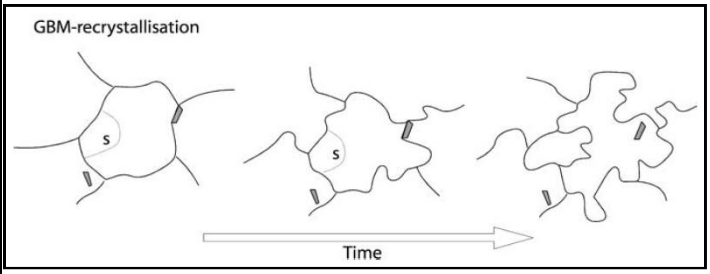

b.

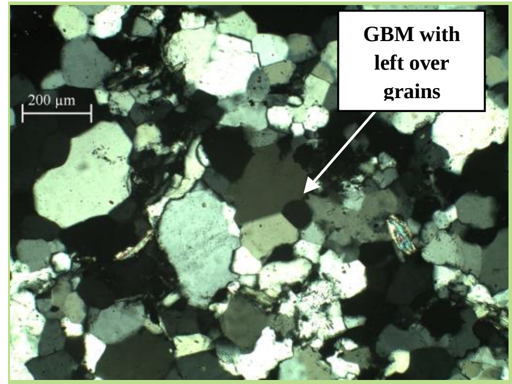

Figure 5.4: (a) Schematic sketch showing stages of Grain boundary recrystallization (GBM), in which grain boundaries become highly mobile and may sweep through entire crystal to remove dislocations. Subgrain rotation also occurs, where grain boundaries (s) are transformed into another grain boundary. Figure 5.4a is after Passchier and Trouw, 2005; P.42. (b) Photomicrograph of quartzite showing GBM recrystallization with left over grains.

5.2.4 Grain Boundary Area Reduction (GBAR)

Grain boundary area reduction is dominant phenomenon observed in quartzites of Narukot, Wadli, Wav and Rustampura. The quartz grains in these quartzites show reduction in free inter-granular space and decrease in total surface area along with increase in grain size. This grain growth is result of annealing, wherein the small grains resorb to form coarser grains with straight boundaries (Fig. 5.5a). The quartz grains show undulose extinction and are largely polygonal with the presence of triple point between adjacent grains having 120° interfacial angle (Fig. 5.5b).

a.

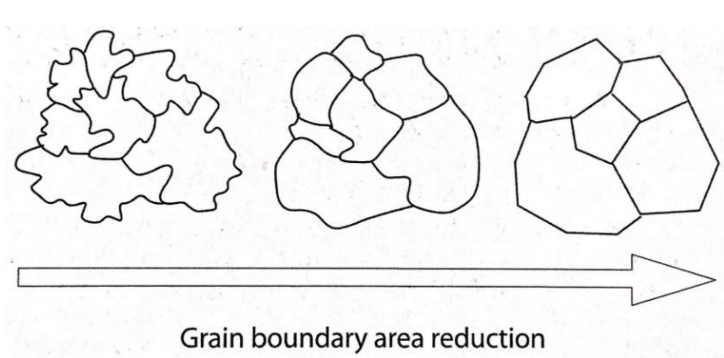

b.

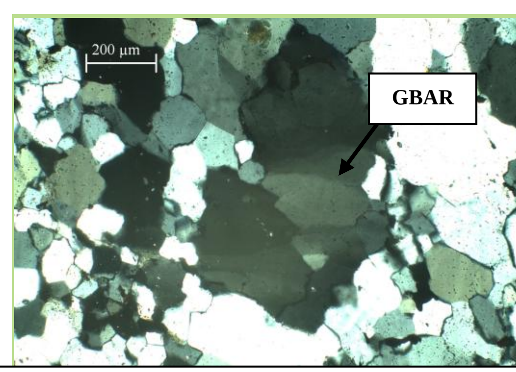

Figure 5.5: (a) Schematic sketch showing development of Grain Boundary Area Reduction recrystallization (GBAR), in which smaller grains resorb together to form larger grain by reducing the surface area of the grain boundary. Figure 5.5a is after Passchier and Trouw, 2005; P.51. (b) Photomicrograph of quartzite showing GBAR recrystallization, the present feature show anomalous undulose extinction.

5.2.5 Discussion

In quartzites, the microstructures, alluded to above show distinct variation in parameters such as grain size, grain shape, free internal energy and extinction. Such distinct microstructural variability has been observed in quartzites from Bamankuwa in the west to Narukot in the east of the Champaner Group, in the form of sequential development of microstructures viz. Bulging recrystallization (BLG), Subgrain rotation recrystallization (SGR), Grain boundary migration recrystallization (GBM) and Grain boundary area reduction (GBAR). In western part the quartzite reveal BLG, SGR and GBM mechanisms with the presence of straight extinction, whereas in the eastern part quartzite discloses GBAR as a dominant process due to high temperature conditions along with undulose extinction.

In the extreme west of the Champaner Group, where it is concealed by the cover of Deccan traps, grain size is found to be fine having irregular grain shape with high free internal energy. BLG is the dominant process in this region. Prograding towards the central part of the Champaner Group, the grains tend to increase and become moderate in size with inequigranular to seriate inter-lobate in shape. This gradual increase in grain size indicates reduction in free internal energy, leading to development of microstructures viz. SGR and GBM. The quartzites closer to Godhra granite in the northern, eastern and southern fringes represent maximum increase in grain size with inequigranular polygonal shape having straight boundaries and triple points. Such coarseness implies thermal maxima of the plutonic intrusive mass along with low free internal energy causing GBAR mechanism. The quartz grains in quartzites, in vicinity of the granite, show undulose extinction. This anomaly signifies that though the temperature was extravagant, there existed high strain rate which did not allow mineral to remove its dislocations. It substantiates that the upwelling granitic mass provided high stress along with heat to display undulose extinction in quartz grains within quartzites located nearer to granite. Conclusively, the post deformational sustained heat of Godhra granite emplacement at the end of the orogeny and induced deformational stresses are the main factors for development of these microstructures.

5.3 Shear Induced Microstructures (SIMs)

Microstructures that develop on account of shearing essentially within the shear zone are termed as Shear Induced Microstructures (SIMs). Moreover, the rocks formed in such high-strain zones are the mylonites (derived from Greek work meaning ‘a mill’). Due to the process called “mylonitization” the rock experiences “milling” (Lapworth, 1885). The two major components of the rock include (i) the porphyroclasts and (ii) the matrix. On account of ductile shearing these rocks display significantly recrystallization of matrix and are classified according to the percentage of matrix as compared to the porphyroclasts (Spry, 1969; Sibson, 1977b; Scholz, 1988; Schmid and Handy, 1991). The rocks 10-50% of matrix are termed as protomylonites; with 50-90% of matrix as mylonites or meso-mylonites and over 90% of matrix as ultramylonites or phyllonites.

The role of shear sense indicators within mylonites is of significant importance in delineating direction of movement i.e. sinistral or dextral, normal or reverse or sense of shear. These shear sense indicators include (i) displacement of markers (ii) foliation curvature (iii) shear band cleavage including C/S fabrics (iv) mantled porphyroclasts (v) mineral fish (vi) quarter structures (vii) lattice preferred orientation. The porphyroclasts which serve as a reference for displacement are commonly feldspar, garnet, micas, hornblende and pyroxenes. The presently known examples forming mineral fishes are biotite, tourmaline, K-feldspar, garnet, plagioclase, staurolite, kyanite, amphibole, hypersthene, diopside, apatite, rutile, hematite, prehnite, leucoxene, sillimanite, olivine and quartz.

The present section aims to describe varieties of shear sense indicators preserved within phyllite-mylonites of the Narukot region. Being phyllite, itself a fine grained rock, mineral aided shear sense indicators are not well developed, however, in such condition ore mineral (comparatively brittle) are used for the present study. This ore mineral displayed as opaque under optical microscope portrays mantled porphyroclasts and fishes varieties, which are important in determining the shear senses. Mineral chemistry acquired through Electron Probe Micro Analyser (EPMA) studies reveals that the ore mineral variety is ilmenite (Figs. 5..6a-b); (Table. 5.1), which shows mantled porphyroclast systems include σ and δ of stair stepping variety and φ type porphyroclasts with strain shadows. All variety of fishes of opaque from Group 1- 6 have been recognised which gives reliable sense of shear. Other important microscopic shear sense indicators include quarter structures and pinch and swell microstructures. The later part of this section discusses probable reasons for the development of these microstructures.

a.

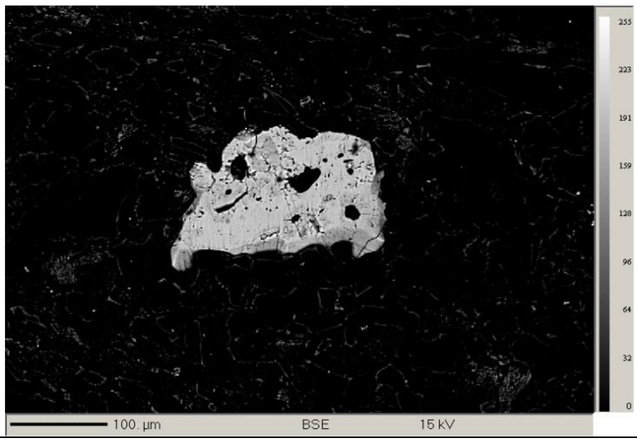

b.

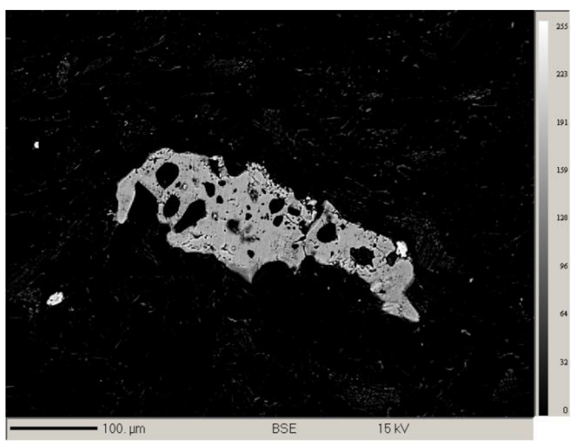

Figure 5.6: Back-scattered electron image of ilmenite, a) sub-rounded and b) elongated with trails on both sides. The ilmenite exhibit single grain in both the cases.

EPMA Analysis of ilmenite

	Phyllite Samples		
Rock no	MAL1	MAL2	MAL3
TiO2	53.80	54.53	51.89
Cr2O3	0.025	0.00	0.00
Al2O3	0.00	0.00	0.034
Nb2O5	0.00	0.00	0.00
FeO	41.99	41.61	40.00
MnO	1.99	2.04	1.69
MgO	0.027	0.007	0.016
CaO	0.00	0.00	0.047
SiO2	0.096	0.007	3.37
Total	97.93	98.21	97.06
Ions on the basis of 6 (O)			
Ti	2.061	2.076	2.071
Cr	0.001	0.000	0.000
Al	0.000	0.000	0.002
Nb	0.000	0.000	0.000
Fe	1.789	1.761	1.775
Mn	0.086	0.088	0.076
Mg	0.002	0.001	0.001
Ca	0.000	0.000	0.003
Si	0.005	0.000	0.179

Table 5.1: Mineral chemistry data of ilmenite from three phyllite samples.

5.3.1 Shear Band Cleavage including S-C fabric

A preferred orientation of mica minerals getting transacted at a small angle by sets of sub-parallel minor slippages are known as shear bands and the group of such minor shears is termed as Shear Band Cleavage (Roper, 1972; White, 1979b; Gapais and White 1982). Shear band cleavage are also termed as extensional crenulation cleavage (Platt and Vissers, 1980). Two varieties of shear band cleavage are known (i) C-type and (ii) C'-type (Berthe et al., 1979a,b) (C= French term Cisaillement, meaning Shear) (Fig. 5.7a). The former develops parallel to the shear zone, while the latter is oblique to the shear zone boundary. In case of C'-type, the angle between shear bands and the shear zone margin is 15-35^{o} (Dennis and Secor, 1987; Passchier, 1991b; Blenkinsop and Treloar, 1995). In case of the

Narukot phyllites, both the varieties of the shear bands have been identified. The C-type shear band is having sub-parallel relationship with the shear zone boundary.

The C plane comprises mica minerals, whereas the S plane (S= Schistosite, meaning Schistosity) is dominated by quartz. Majority of the C-type bands are anastomosing, long and wavy (Fig. 5.7b). At places these bands are found to have developed along the M-domain (mica rich-domain) of the earlier compressional crenulation cleavages (Fig. 5.7c). In case of C'-type shear band, the angle between C' and shear zone boundary is around 27-32^{o}.The phyllite-mylonite consisting C'-type shear band prominently display the compositional banding. The areas within the slide, which are dominantly composed of mica minerals exhibit the C'-type shear band cleavage (Figs. 5.7d-f). However, for C and C'-type, interpretation of shear direction suggests top-to-east senses of ductile shear.

5.3.2 Mantled Porphyroclasts

The major component within the mylonites called porphyroclast, is the large single grain surrounded by fine-grained matrix. Commonly known examples of porphyroclasts are feldspars, orthopyroxenes and dolomites within matrix of quartz-feldspar-mica, peridotite and calcite, respectively. When these porphyroclasts are associated with the polycrystalline rims of different composition than matrix, such assemblages are termed as Porphyroclasts Systems. If the material in the rim is same as that of the porphyroclasts, the rim is called as mantle and the overall microstructure is referred as Mantled Porphyroclast or Mantled Clast (Passchier and Trouw, 2005). Depending on the orientation in the mylonite, the fine grained mantle can be deformed into wings or trails (Passchier and Simpson, 1986). In case of variation in the composition of the rim and the porphyroclast, the adjacent tapering regions are termed as "Strain Shadows". In such situation, the overall microstructure is treated as porphyroclasts with strain shadows.

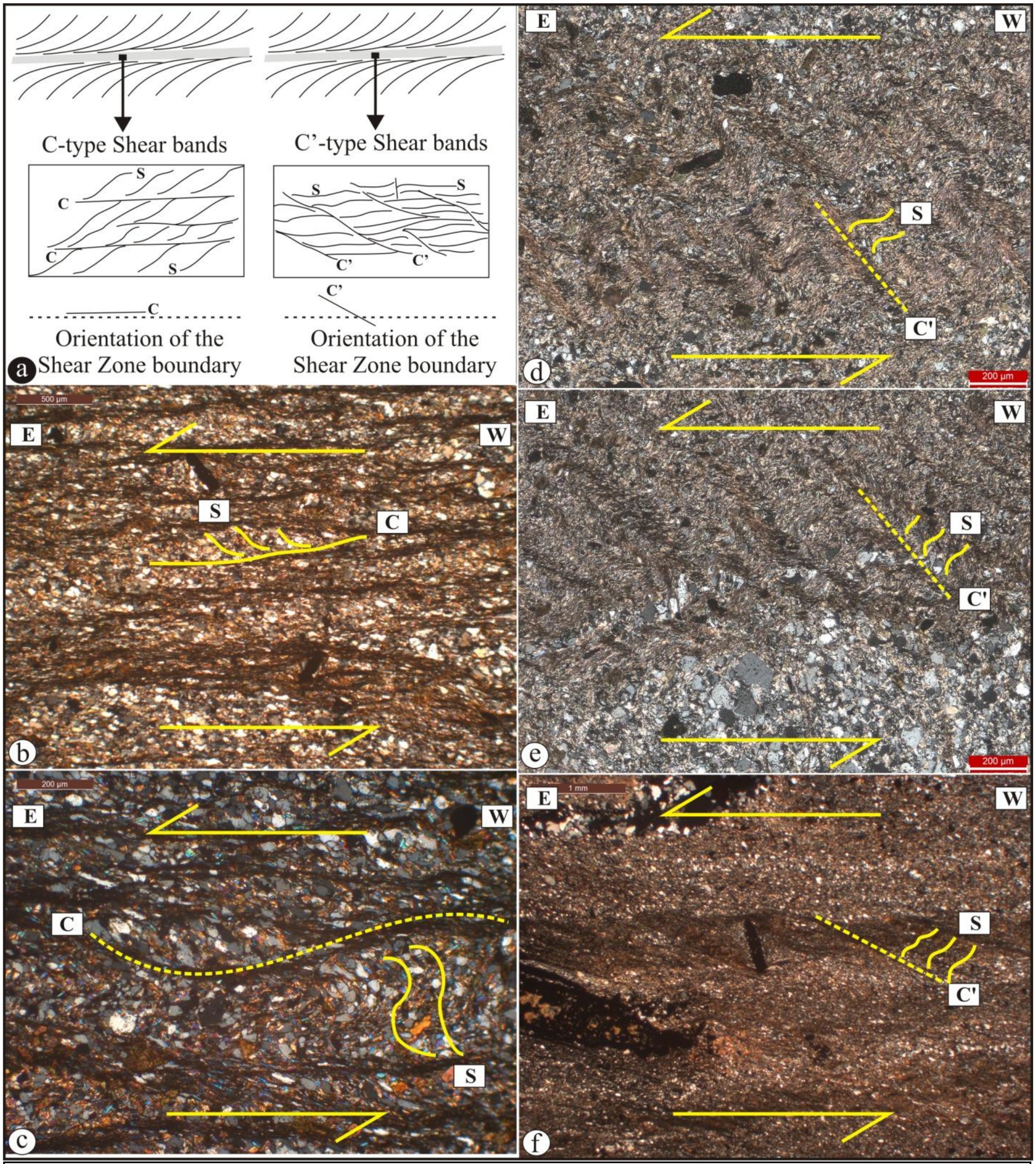

Figure 5.7: (a) Two varieties of shear band cleavages have been drawn C and C'. The former is parallel to the shear zone boundary where as the latter is oblique. This sketch is modified after Passchier and Trouw, 2005; p.128); Photomicrographs in XPL of phyllite-mylonite showing (b) anastomosing C-type shear bands; (c) compressional crenulations getting sheared to form extensional crenulations; (d-f) M-domain and Q-domain within the phyllite-mylonite. C' plane has been developed within the mica rich zone and is oblique to the shear zone boundary. Yellow half-arrows indicate the shear direction top-to-east.

According to the classification of mantled porphyroclasts, designated on the basis of the shape of the trails (Hanmer, 1984b; Passchier and Simpson, 1986; Hooper and Hatcher, 1988); they are distinguished into four principal types. Viz. (i) φ -type (Phi), (ii) σ-type (Sigma), (iii) δ-type (Delta) and (iv) Complex mantled clasts (Fig. 5.8). In φ -type (Phi) mantled porphyroclast, there is tapering of mantles on either side of the porphyroclasts. The edges of the trails lie at same elevation on both the sides. σ-type (Sigma) mantled porphyroclats consists of wider mantles with two planar and curved faces, defining an internal asymmetry. The tips of the trails lie at different elevation on both the sides with respect to the imaginary reference line drawn from the centre of the porphyroclats and referred as “Stair-stepping” (Lister and Snoke, 1984). δ-type (Delta) mantled porphyroclasts have narrow wings and could be of both stair-stepping or non-stair-stepping varieties. Complex mantled clasts consist of more than one set of trails (Passchier and Trouw, 2005). Among all types of the porphyroclasts, σ and δ are commonly useful in deciphering the shear direction.

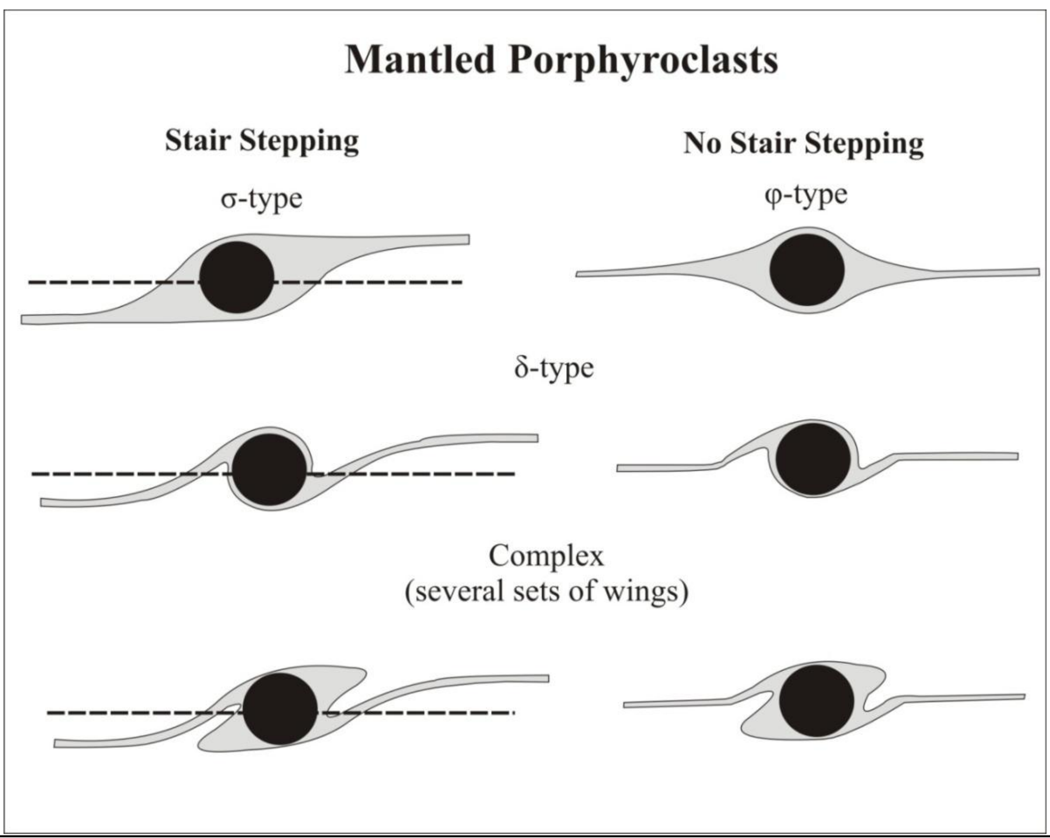

Figure 5.8: Classification of mantled porphyroclasts having dextral shear senses (after, Passchier and Trouw, 2005; p. 133).

In case of the phyllite-mylonites from the Narukot region, ilmenite as an opaque mineral is used as uncommon porphyroclast. Various mantled porphyroclasts such as σ, δ of stair stepping variety and φ type porphyroclasts with strain shadows have been identified. The φ type porphyroclasts consist of trails at same elevation on both sides and display variety of shapes such as “oval shaped” (Figs. 5.9a-b); “fish headed” with swallowed quartz grain (Figs. 5.9c-d); “amoeboid shaped” having irregular boundary (Figs. 5.9e-f); “oblong shaped” (Figs. 5.9a-b) and “hatched circular shaped” with strain shadows (Figs. 5.10c-d). However, among these varieties, quite a few display prominent top-to-east shear senses that too based on the surrounding S-C fabric. σ and δ mantled porphyroclasts of stair stepping variety are found to be preserved within the phyllite-mylonites of the Narukot region. The σ-type porphyroclasts show wider mantles with two curved surfaces on the either side of the porphyroclasts having internal asymmetry. The tips of the trails are found to be located at different elevation with respect to the reference line drawn at the centre of the porphyroclasts (Figs. 5.10e-f). These trails are parallel to the C and C’ planes of the shear band cleavage present within the phyllite mylonites of the region (Figs. 5.11a-f). The δ-type mantled porphyroclasts have narrow mantles with the trails developed on the opposite side of the rotated opaque. These trails are often found to be truncated along the C’ planes of the shear band cleavage. The overall shear represent reliable top-to-east shear senses (Figs. 5.12a-b).

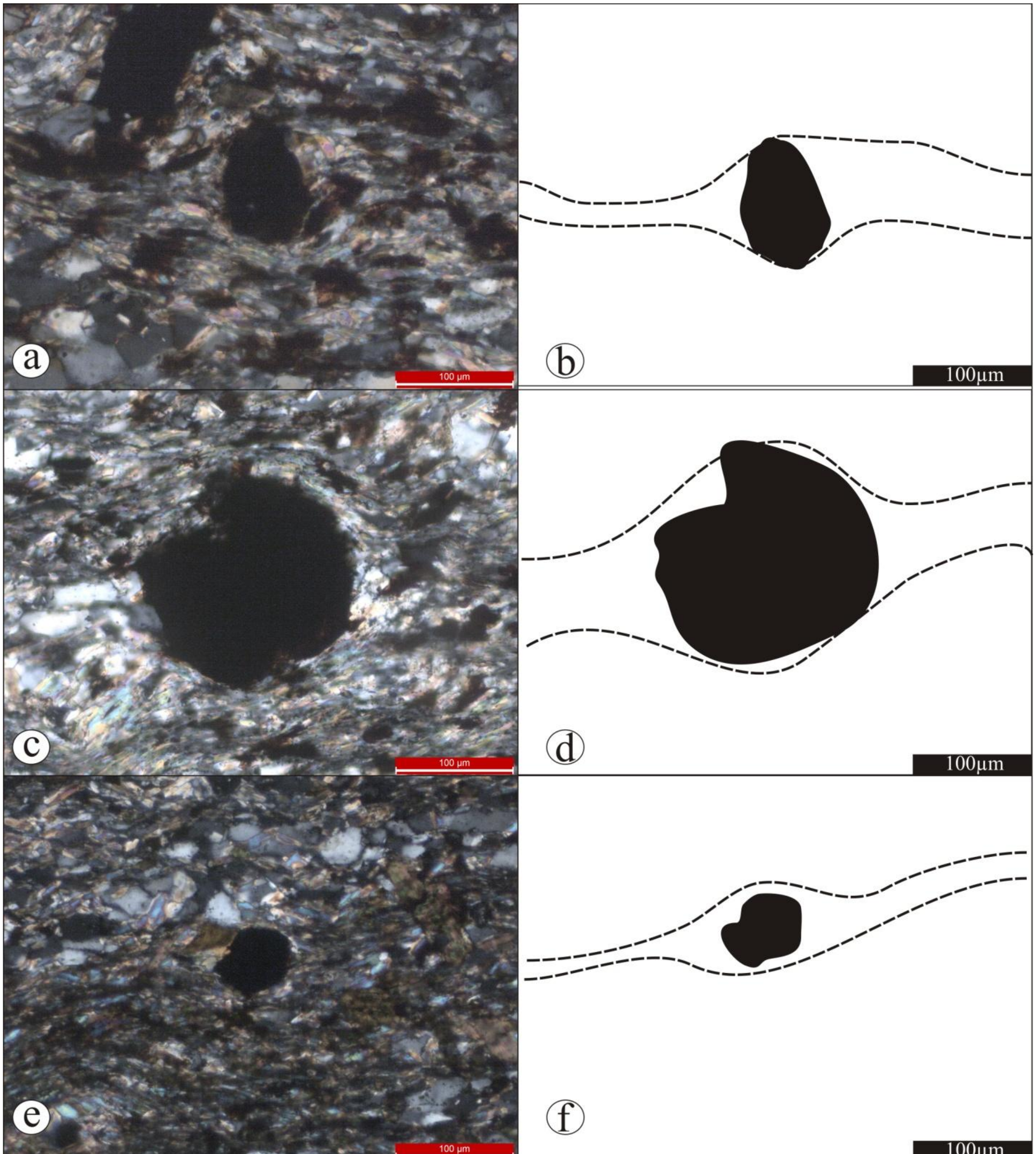

Figure 5.9: Photomicrographs in XPL with lined sketch of phyllite-mylonite showing (a,b) “Oval shaped” φ-type mantled porphyroclasts with tapering trails at same elevation on both sides; (c,d) “Fish head shaped” φ-type mantled porphyroclasts with swallowed quartz grain; (e,f) “Amoeboid shaped” φ-type mantled porphyroclasts having irregular boundary.

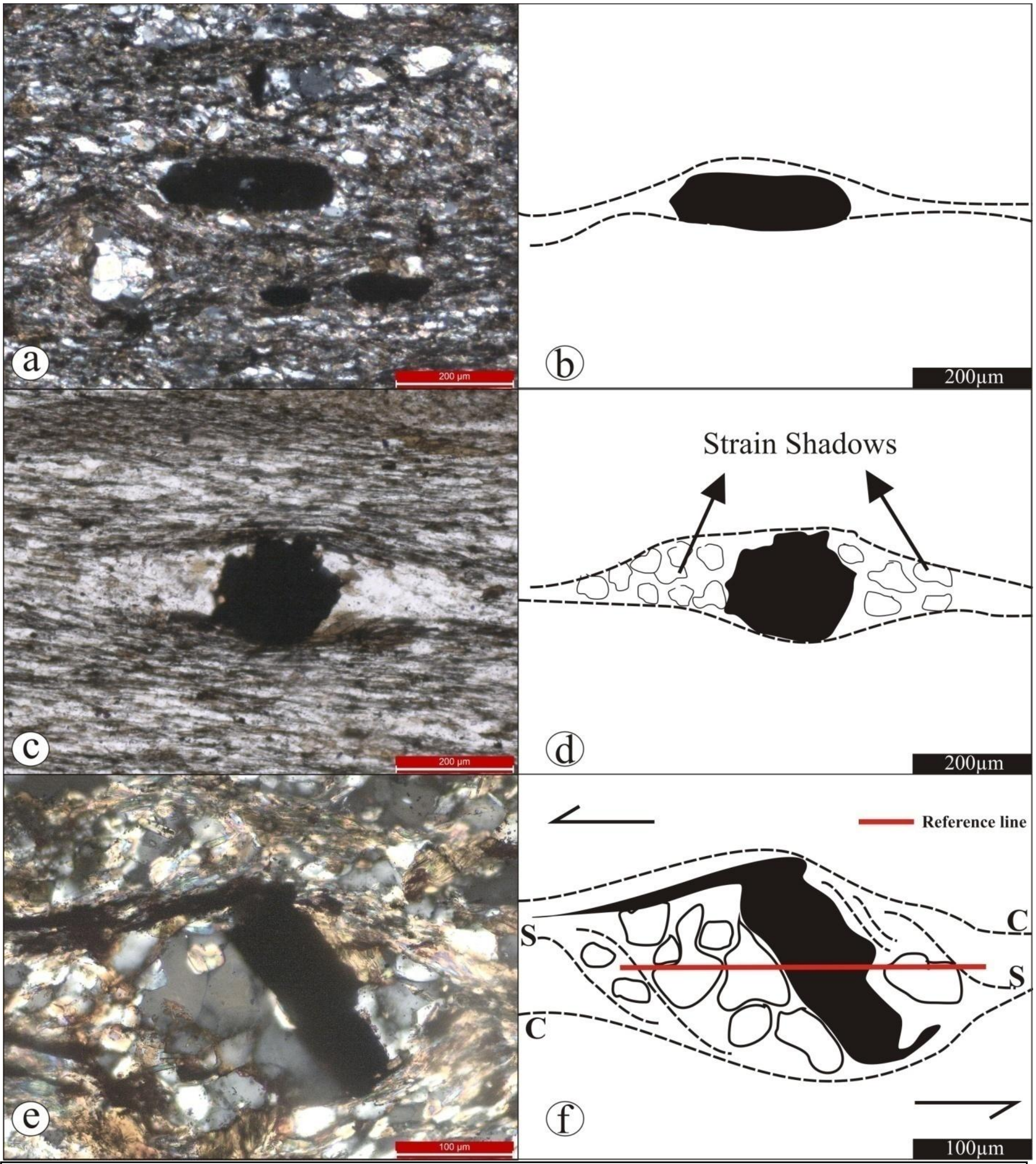

Figure 5.10: Photomicrographs in XPL/ PPL with lined sketch of phyllite-mylonite showing (a,b) “Oblong shaped” φ-type mantled porphyroclasts with tapering trails. The upper half of the photomicrograph display prominent S-C fabric; (c,d) “Hatched circular shaped” φ-type mantled porphyroclasts with strain shadows. Quartz is the main mineral developed within the shadow free zone; (e,f) σ-type mantled porphyroclasts of stair stepping variety. The tips of the trails are at different elevation with respect to the red reference line drawn at the centre. Black half-arrow within the sketch indicate the shear direction top-to-east.

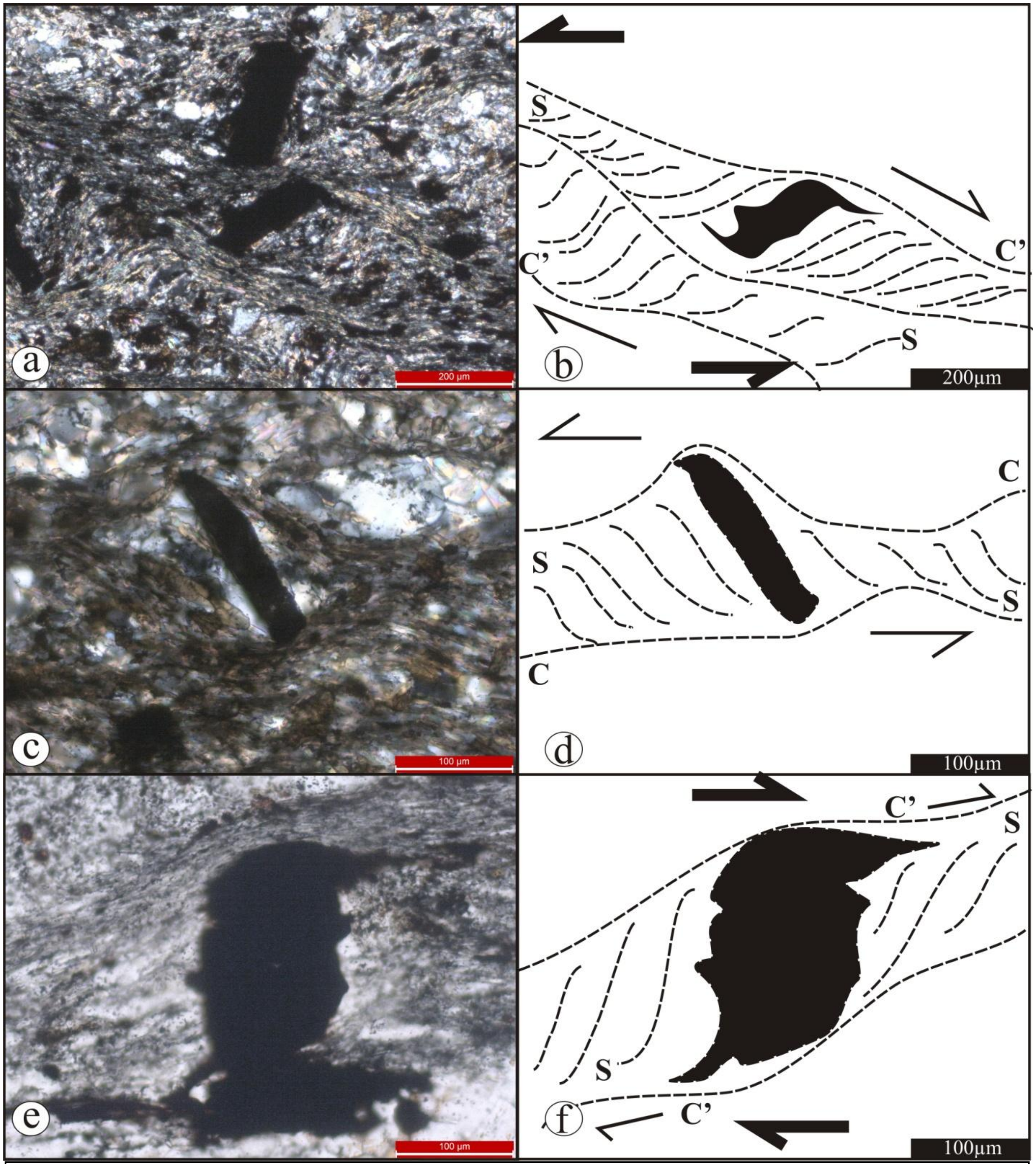

Figure 5.11: Photomicrographs in XPL/ PPL with lined sketch of phyllite-mylonite showing (a-f) σ-type mantled porphyroclasts of stair stepping variety. The tips of the trails are parallel to the C and C' planes of the shear band cleavage present within the phyllite mylonites. Thickened black half-arrows within the sketch indicate the shear direction top-to-east, whereas thinned black half-arrows indicate the shearing long C' plane, which is oblique to the shear zone boundary.

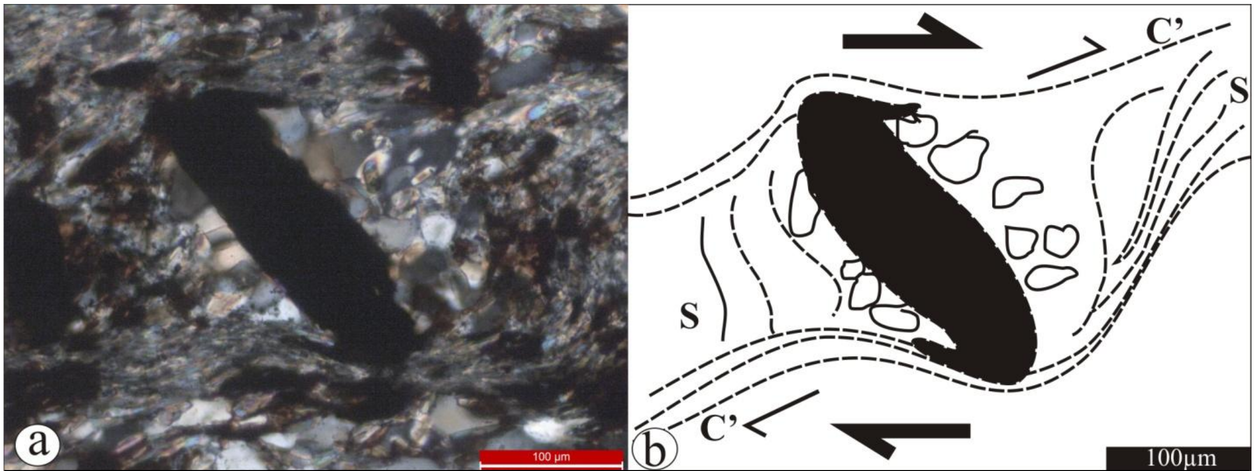

Figure 5.12: Photomicrographs in XPL with lined sketch of phyllite-mylonite showing (a,b) δ-type mantled porphyroclasts of stair stepping variety. The trails are developed on the opposite side of the rotated opaque and often found to be truncated along the C' planes, which is oblique to the shear zone boundary. Thickened black half-arrows within the sketch indicate the shear direction top-to-east, whereas thinned black half-arrows indicate the shearing long C' plane.

5.3.3 Mineral Fishes

Mineral Fishes, usually observed under optical microscope are sheared and commonly asymmetric grains or clusters of grains (Mukherjee, 2011a). These fishes are lozenge-shaped porphyroclasts with single crystals embedded within fine grained matrix (ten Grotenhuis et al., 2002; ten Grotenhuis et al., 2003; Mukherjee and Pal, 2000). The characteristic features show their longest dimension at a small angle with respect to the mylonitic foliation. The present concept originated from 'mica fish', where they are bounded by micro-shear zones that produced by crystal-plastic deformation/ brittle deformation/ fracturing parallel to their (001) cleavage planes/ pinching at the corners (Lister and Snoke, 1984; Mukherjee, 2011) and has been considered as strain insensitive S-fabrics (Davis and Reynolds, 1996). These fishes are used to decipher shear senses at various tectonic settings viz. from a rift zone by (Kula et al., 2007); from a continent–continent collision zone by (Mukherjee and Koyi, 2010a) and from a transform fault zone by (Zhu et al., 2007).

Besides mica, commonly known examples of other minerals that possess fish morphology are tourmaline, k-feldspar, garnet, plagioclase, staurolite, kyanite, amphibole, hypersthenes, diopside, apatite, rutile, hematite, prehnite (Mancktelow et al., 2002; ten Grotenhuis et al., 2003), leucoxene

(Oliver and Goodge, 1996), sillimanite (Pennacchioni et al., 2001; Mancktelow et al., 2002), olivine (Mancktelow et al., 2002) and quartz (Bestmann et al., 2000, 2004; ten Grotenhuis et al., 2003). Ten Grotenhuis et al, (2003) proposed a morphological classification scheme for mica fish, which has been divided into six groups, viz. (1) lenticular, (2) lenticular with points inclined towards the foliation, (3) rhomboidal with cleavages parallel to the longest side of the fish, (4) rhomboidal with cleavages parallel to the shortest side of the fish, (5) fish with small aspect ratio and curved tails, and (6) fish with high aspect ratio and stair-stepped tails (Fig. 5.13).

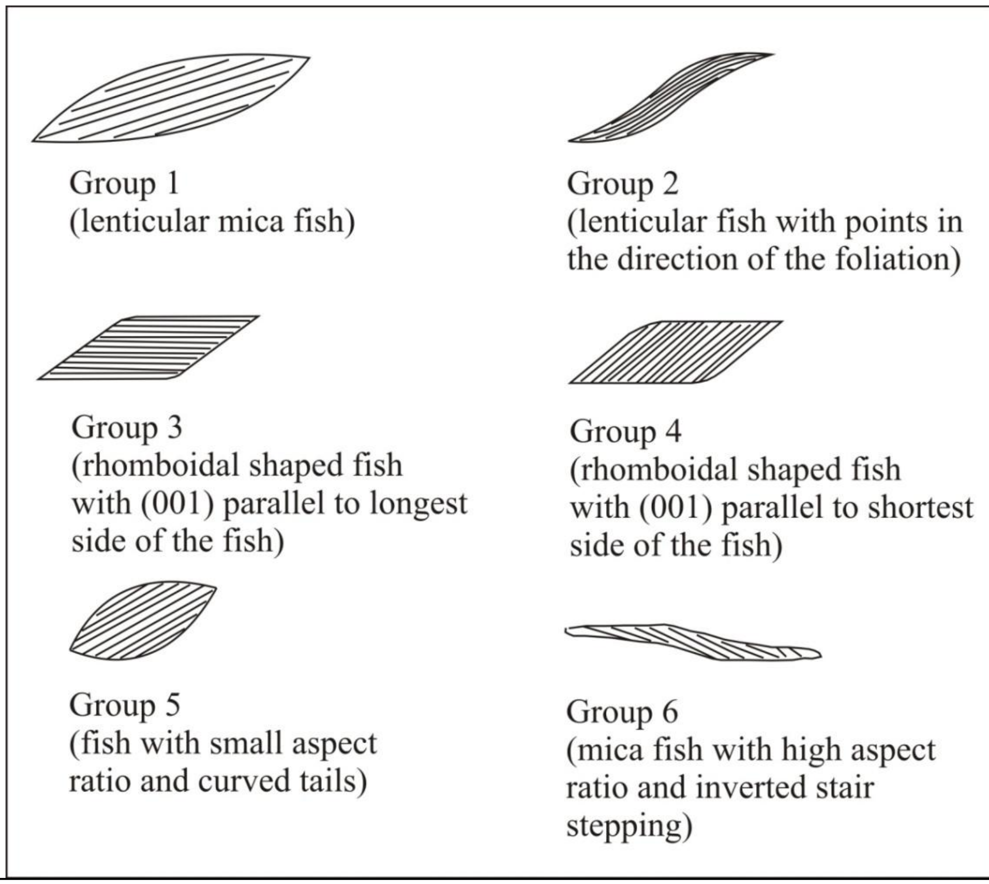

Figure 5.13. Morphology of mica fish, groups 1-6 (after, ten Grotenhuis et al., 2003)

The phyllite-mylonites belonging to the Narukot region show all varieties of opaque fishes. Being opaque devoid of any cleavage planes the morphology has been treated as fish type morphology.

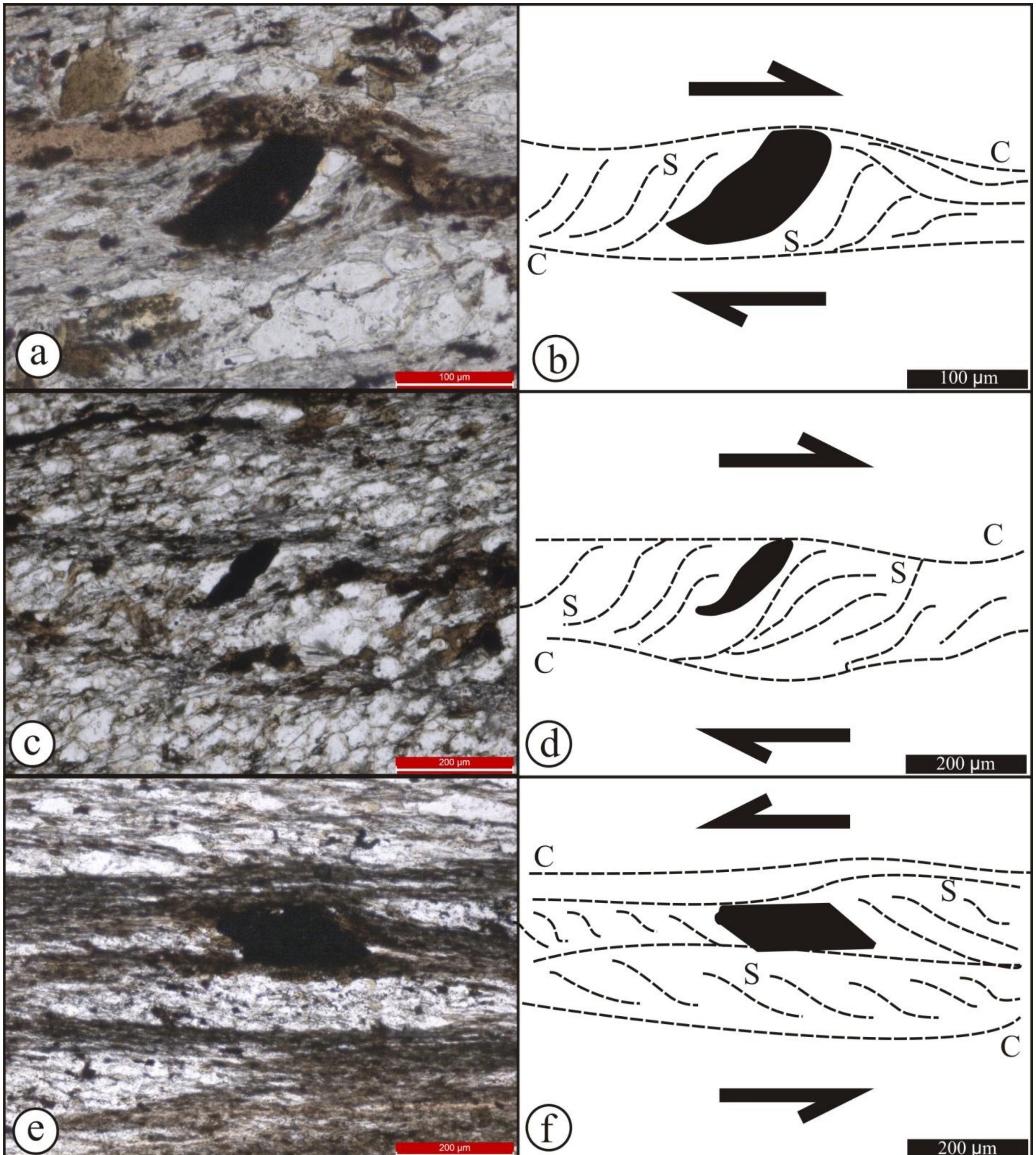

Figure 5.14: Photomicrographs in PPL with lined sketch of phyllite-mylonite showing (a,b) Group 1 opaque fish (R= 2.65; $\alpha = 42^o$); (c,d) Group 2 opaque fish (R = 4.33; $\alpha = 45^o$); (e,f) Group 3 opaque fish (R = 2.66; $\alpha = 22^o$). Thickened black half-arrows within the sketch indicate the shear direction top-to-east.

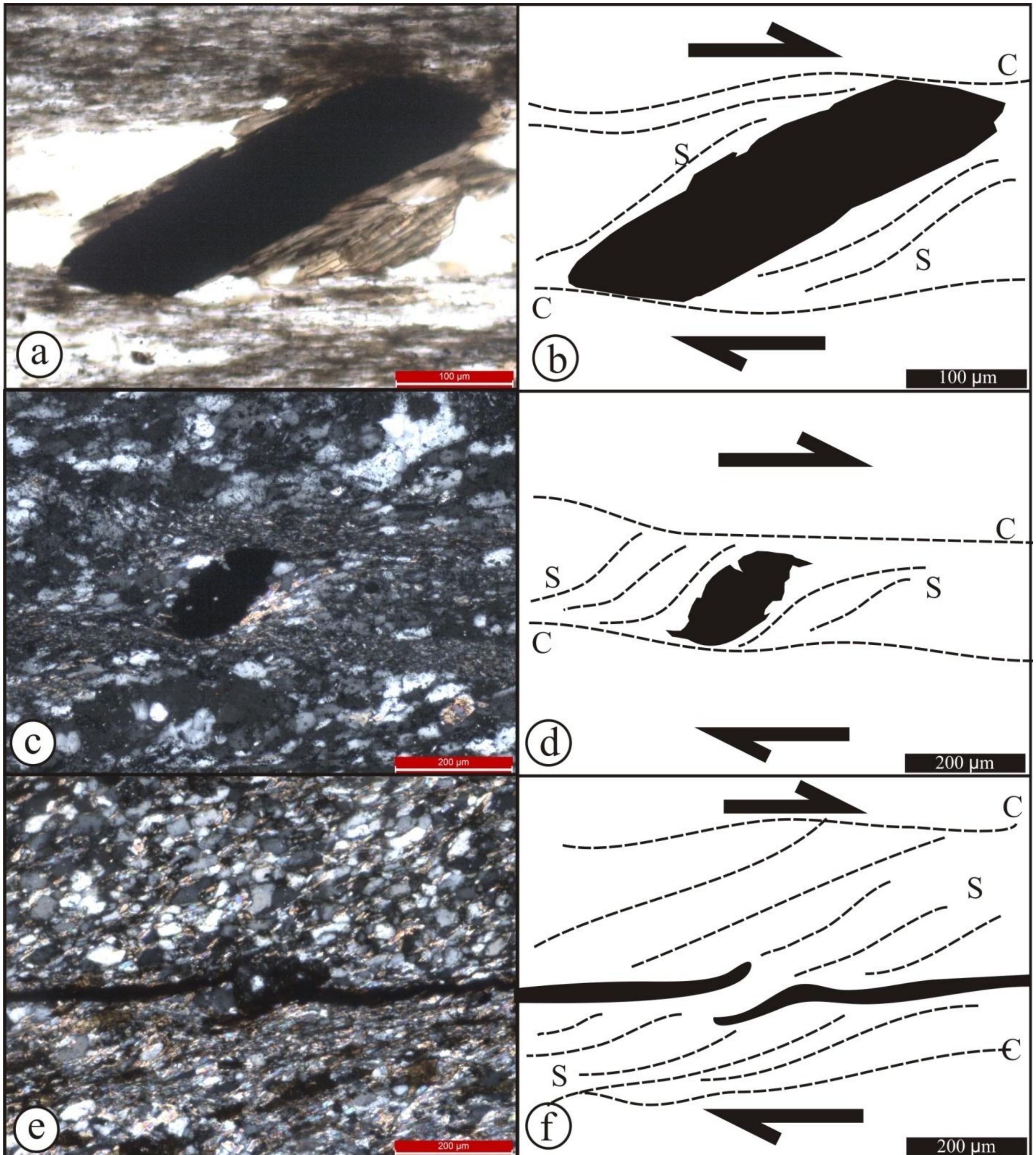

Figure 5.15: Photomicrographs in PPL/XPL with lined sketch of phyllite-mylonite showing (a,b) Group 4 opaque fish (R= 4.5; α = 42^{o}); (c,d) Group 5 opaque fish (R = 2; α = 31^{o}); (e,f) Group 6 opaque fish (R = 14; α = 12^{o}). Thickened black half-arrows within the sketch indicate the shear direction top-to-east.

The Group 1 type opaque fish of lenticular variety consists curved sides with sharp tips (Figs. 5.14a-b). The tips of the present variety are found to parallel to the mylonitic foliation having C-planes. The aspect ratio 'R' calculated using the formula R= D T_{max}^{-1}, (where D = diagonal long axis measurement of the fish and T_{max} = the orthogonal thickness measurement with respect to the mineral fish boundary) and α = angle between T_{max} and sheared plane, suggest R= 2.65; α = 42^{o}. In case of Group 2 opaque fish the tips are curved having R = 4.33; α = 45^{o} (Figs. 5.14c-d). The Group 3 opaque fish is parallelogram with straight sides. The longest axis of the present fish is found to be parallel with the C-planes having R = 2.66; α = 22^{o} (Figs. 5.14e-f). The Group 4 opaque fish is too parallelogram shaped but having shortest axis parallel to the mylonitic foliation C (Figs. 5.15a-b). The aspect ratio R and α of Group 4 opaque fish is 4.5 and 42^{o}, respectively. The Group 5 opaque fish display curved sides as well as tips in a manner that they lay on the different line as the upper and lower parts of the central opaque fish (Figs. 5.15c-d). The aspect ratio of this variety is R = 2 with α = 31^{o}. Finally, Group 6 opaque fish is of elongated snake shaped often found to be truncated by C planes. The R value of the Group 6 fish is 14 having α angle of 12^{o} (Figs. 5.15e-f).

5.3.4 Quarter Folds

As per definition (sensu-stricto), "quarter structures are those structures in which porphyroclasts without mantles show an asymmetric distribution of microstructures over the four quarters defined by the foliation and its normal" (Hanmer and Passchier, 1991). Moreover, "microfolds in the quarters that lie in the extensional direction are known as quarter folds" (Passchier and Trouw, 2005). The phyllite-mylonites from the Narukot area represent quarter folds developed on account of top-to-east sense of ductile shear. The external fabric display micro-folding along alternate quadrants, possibly resulted due to the rotation of opaque (Figs. 5.16a-f).

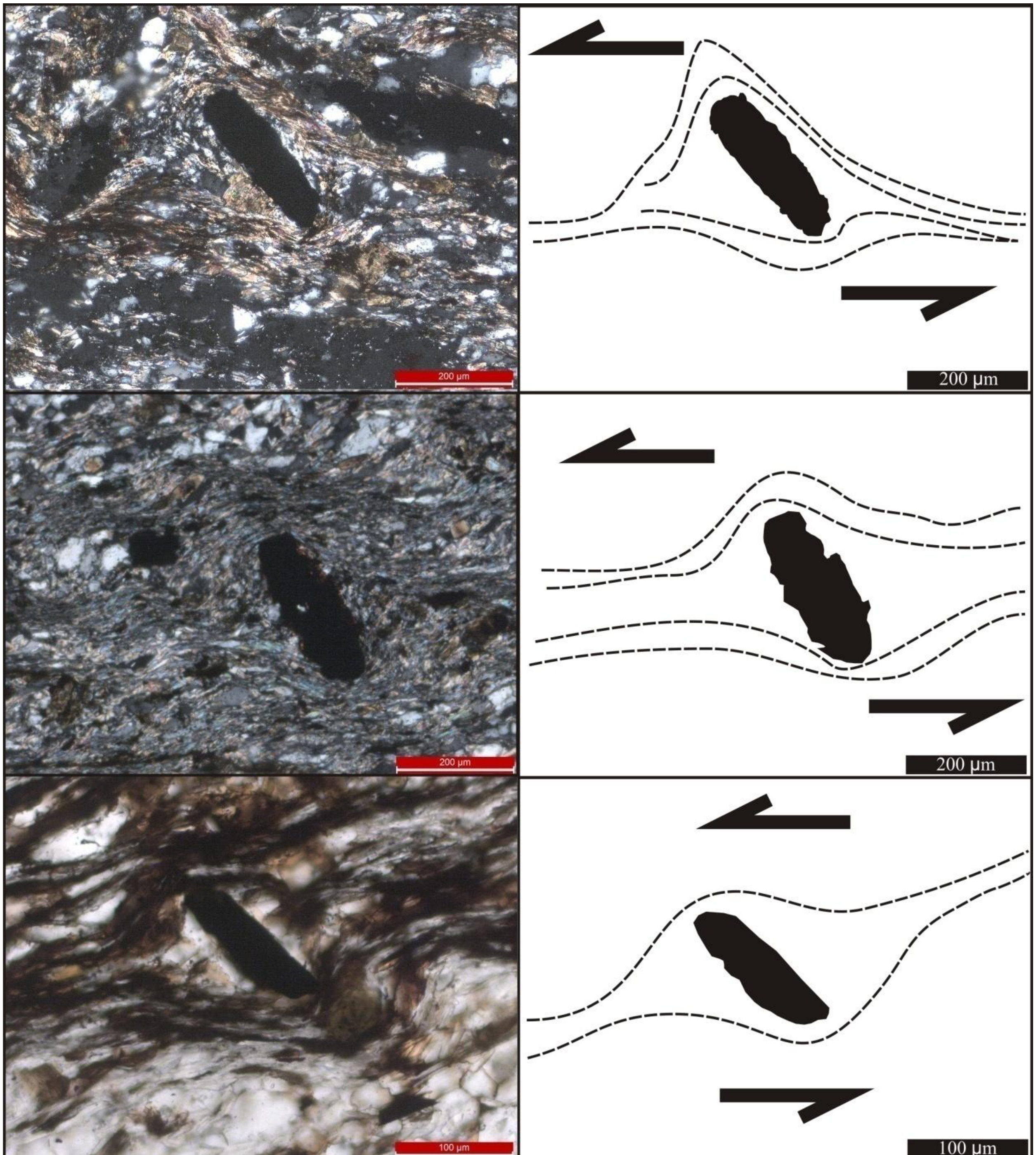

Figure 5.16: Photomicrographs in PPL/XPL with lined sketch of phyllite-mylonite showing oblong shaped opaque porphyroclasts without mantles having top-to-east rotation. Micro-folding along alternate quadrants has developed generating asymmetric folds of external fabric. Thickened black half-arrows within the sketch indicate the shear direction top-to-east.

5.3.5 Pinch and Swell microstructure

Boudins (meaning from French: boudin = sausage) are the series of rock fragments attached by thin necks to project an appearance of a string of sausages (Lohest et al., 1908). They form essentially in competent units on account of layer parallel extension within a weaker matrix, having a size range of regional scale to outcrop scale to micro scale (Goldstein, 1988; Klepeis et al., 1999; St-Onge et al., 2009). Pinch and swell microstructure is the variety of neck boudin or subset of boudins that continues with the difference in thinning at irregular intervals with respect to the original layer thickness (Gardner et al., 2015). Pinch and swell structures have been reported from various tectonic settings and crustal levels (Arslan et al., 2008; Goscombe et al., 2004; Hobbs et al., 2010; Kenis et al., 2004; van der Molen, 1985). The phyllite-mylonite of the Narukot region preserve within them pinch and swell microstructures. The opaques show variability in terms of their thickness due to contrast in competence with the surrounding matrix (Figs. 5.17a-b).

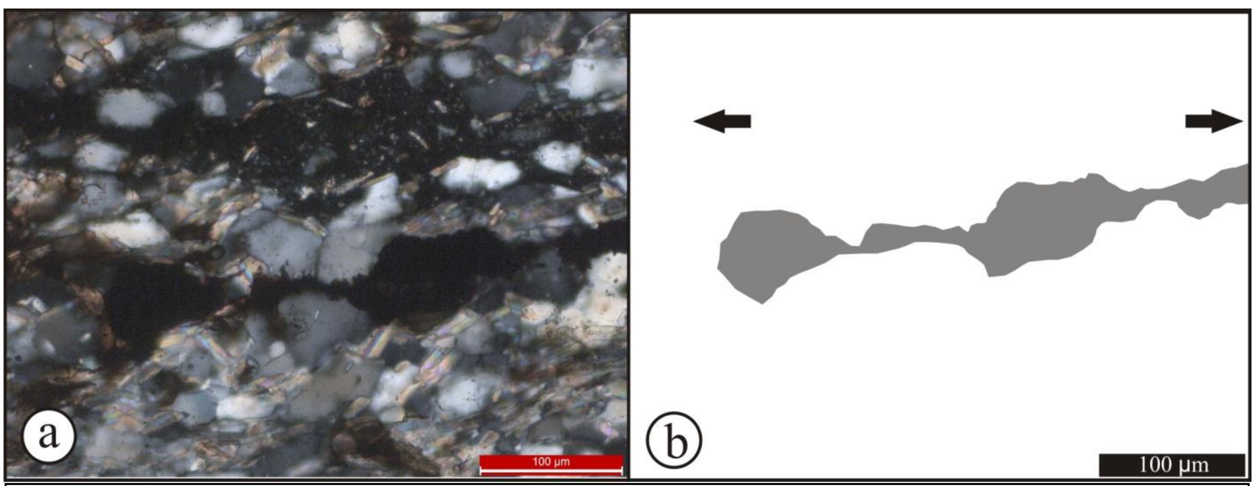

Figure 5.17: (a) Photomicrograph in XPL with (b) lined sketch of phyllite-mylonite showing pinch and swell microstructure in opaque. Black arrows within the sketch indicate layer parallel extension along E-W direction.

5.4 Complex Microstructures (CMs)

Microstructures entrapped within the porphyroblasts display complexity in terms of their origin. Such microstructures are treated as Complex Microstructures (CMs). The andalusite hornfels, north of Narukot near Wadek, exhibit deflection fold structure on a micro-scale. 2.2 cm long andalusite porphyroblast within the hornfels show serrated margin with recrystallized matrix (Figs. 5.18a). The inclusions within the andalusite are primarily quartz but often show presence of muscovite due to the process of muscovitization. Bell and Rubenach (1980) and Bell (1981) described microstructures developed during inter and syn-tectonic event referred to as “millipede” microstructure. Passchier and Speck (1994) coined such structures as deflection-fold structure. Johnson and Moore (1996) introduced the concept of Oppositely Concave Microfolds (OCMs) in which these structures are an effect of foliation deflection adjacent to a rigid porphyroblast. Similar structures have been explained experimentally in homogeneous, non-partitioned flow around rigid objects by (Ghosh and Ramberg, 1976; Masuda and Ando, 1988; Gray and Busa, 1994).

In case of andalusite hornfels, the presence of recrystallized matrix has masked the external fabric of the OCMs. In such situation, the external schistosity has been inferred. Based on the inferred deflection of external fabric it can be said that the top-to-east sense of ductile shear has led to the development of oppositely concave microfolds (Figs. 5.18b). Moreover, inclusions present within the porphyroblast suggest its syn-tectonic origin. Thus it will be more relevant and logical to deduce that the recrystallization of the matrix is a later event than shearing and resultant inclusions are the frozen remnants within the syn-tectonic andalusite.

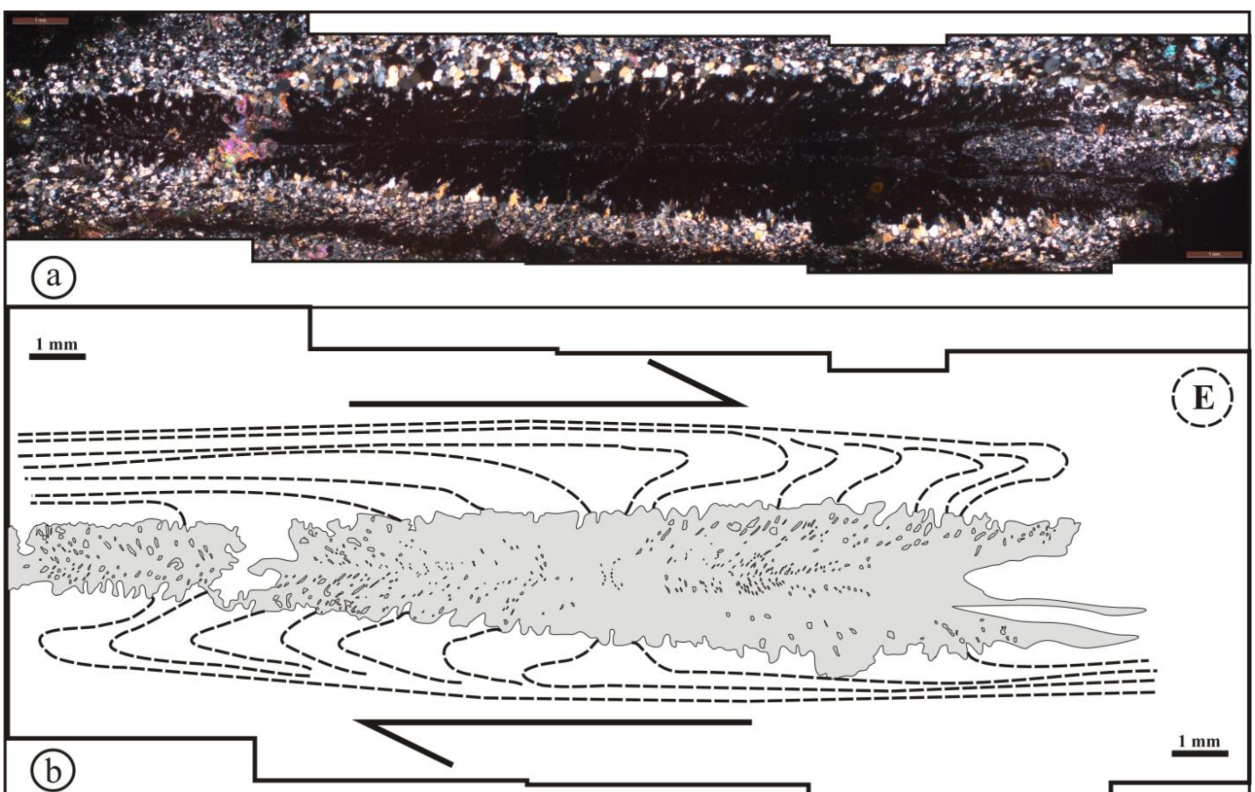

Figure 5.18: (a) Photomicrograph in XPL of andalusite hornfels showing presence of quartz and muscovite inclusions along with the recrystallized matrix. (b) Lined sketch of andalusite porphyroblast having Oppositely Concave Microfolds (OCMs). Dotted lines indicate the inferred form of external fabric based on the inclusion trails. Half arrows exhibit shear sense top-to-east.

5.4.1 Discussion

As mentioned in the Chapter 4 (section 4.9), the Champaner Group has experienced brittle and ductile faults/ shears after the episode of folding. The manifestations of strike slip faults in cross-section have resulted in to top-to-east reverse shears and are mainly concentrated in vicinity of the Narukot dome. Microstructures preserved within phyllite-mylonites of the Narukot region and andalusite hornfels of the Wadek region, reliably give top-to-east sense of movement. The root cause of these faults/ shears are the granites, which emplaced in vicinity of these sequences. The granite emplacement not only caused the deformation perhaps was responsible for coarsening of matrix within these mylonites.

5.5 Granite Microstructures

The detailed microscale observations of granites were carried out to understand the mineralogical, textural and deformational characteristics. Granites can be differentiated based on the grain size, viz. a) fine grained and b) coarse grained granites. Moreover, the deformational characteristics of granites are distinctly observed along with other microscopic features. Total 23 samples of granites were acquired from the field and were subjected to microscale analysis.

The granites of study area represent typical coarse/ fine grained, holocrystalline and hypidiomorphic texture (Figs. 5.19a-c). The coarse grained granites can be classified into two types based on textural variation. The grain size dissimilarity within the coarse grained granites leads to a) porphyritic and b) aphyric variety of textures. The granite frequently represents the poikilitic texture in which the chadacrysts of quartz, biotite, plagioclase and other accessory minerals are enclosed within the oikocryst of K-feldspar (Fig. 5.19d). The other essential minerals are also observed as chadacrysts in subordinate manner. In addition to that the exsolution textures are common in the granites of the study area. The textures such as perthites (intergrowth of sodic and potassic feldspars), microperthites and myrmekite (intergrowth of quartz and potassic feldspar) are observed. The sample collected from Wadek, SE of Valothi and Dev Dungar represents prominent myrmekitic texture, whereas the samples from Sagwa and Zab village exhibit micro-perthites in accordance with the major texture (Figs. 5.19e-f);

(Fig. 5.20a). The sample obtained from Sukhi dam site (Dhanpur) ideally representing myrmekitic, perthitic (flame perthite) and microperthitic textures (Fig. 5.20b) (all locations in the geological map, Fig. 3.1).

The essential mineralogy of granites includes orthoclase, microcline, plagioclase, quartz and biotite where as the accessory mineral phases are hornblende, muscovite, epidote, calcite, chlorite and opaque minerals. Microscopic observation portray that the K-feldspars and the plagioclase feldspars are the dominant mineral phases followed by the quartz and biotite. The biotite content is relatively less in the coarse grained granites of southern and eastern margins of the Champaner Group, whereas it increases in the fine grained varieties of northern and northwestern margins. The hornblende is present in the subordinate amount except near Valothi, where it dominates the occurrence of biotite.

5.5.1 Xenoliths and deformation within granites

As discussed in the chapter-3, geological setting of the study area (section 3.2.6.3), the xenoliths present in the granites, located in and around Champaner Group can be genetically classified in two types, 1) metamorphic xenoliths and 2) granitic xenoliths.

The metamorphic xenoliths are of calc-silicate rock and schistose rock. The calc-silicate rock xenolith is present in the granites of SE of Valothi. They typically show hornfelsic texture (Fig. 5.20c), in response to the hot granitic emplacement into the calc-silicate country rock. The hornblende porphyroblasts within these calc-silictes depict sieve texture. The schistose xenolith obtained from the fine grained granite variety of Sukhi dam site (Dhanpur), display the intercalated layers of quartz and mica minerals (muscovite) (Fig. 5.20d).

The granite xenoliths within the coarse grained granite variety, show distinctive granitic mineralogy and textures (Fig. 5.20e). These xenoliths suggest dominance of plagioclase feldspar over K-feldspars. Biotite, quartz, orthoclase and hornblende are the mineral phases present other than plagioclase feldspar. The biotite content is found to be increased with respect to the coarse grained granite variety. Occurrence of fine grained granite as xenolith within the coarse grained granite is indicative of two phases of granitic emplacement within the study area. Amongst these two emplacement phases the earlier phase is fine grained granite followed by the second phase of coarse grained granite variety.

Deformation microstructures within granite can be classified into two types based on the textural criteria, viz. 1) Low temperature solid state deformation microstructures and 2) High temperature solid state deformation microstructures. The features such as a) undulose extinction in quartz (Fig. 5.20f) and biotite (Fig. 5.21a); b) kinking in biotite (Fig. 5.21b); c) micro-faulting (Fig. 5.21c) and fracturing in crystals (Fig. 5.21d) and d) micro-folds in mica minerals (Fig. 5.21e) suggest that the granite has undergone low temperature solid state deformation, whereas the chess-board extinction pattern in quartz (Fig. 5.21f) is indicative of high-temperature solid-state deformation fabric.

5.6 Time relationship between deformation and metamorphism/ metasomatism

Porphyroblasts usually contain inclusion trails, which are indicative of the structure possessed by external fabric during their growth. Although, the matrix may be modified during later events due to external forces but these rigid porphyroblasts resist inherent inclusion trails from further modification (Passchier and Trouw, 2005) and provide an insight to decode the sequence of deformation events and its relationship with the metamorphic growth. Meta-pelites are the best hosts for the time relationship study; their samples from F_1, F_2 and F_3 dominated region have been acquired. Furthermore, the metapelites present in vicinity of the granitic intrusion have also been analyzed, which gives an overall understanding in terms of the mineral development during various stages of deformation and culminated magmatic event within the Champaner Group. Relationship between deformation and metamorphism/ metasomatism has been established with the help of porphyroblasts matrix relations. The model generated by using the said parameters should be considered as tentative and needs a scope for further in-depth investigation.

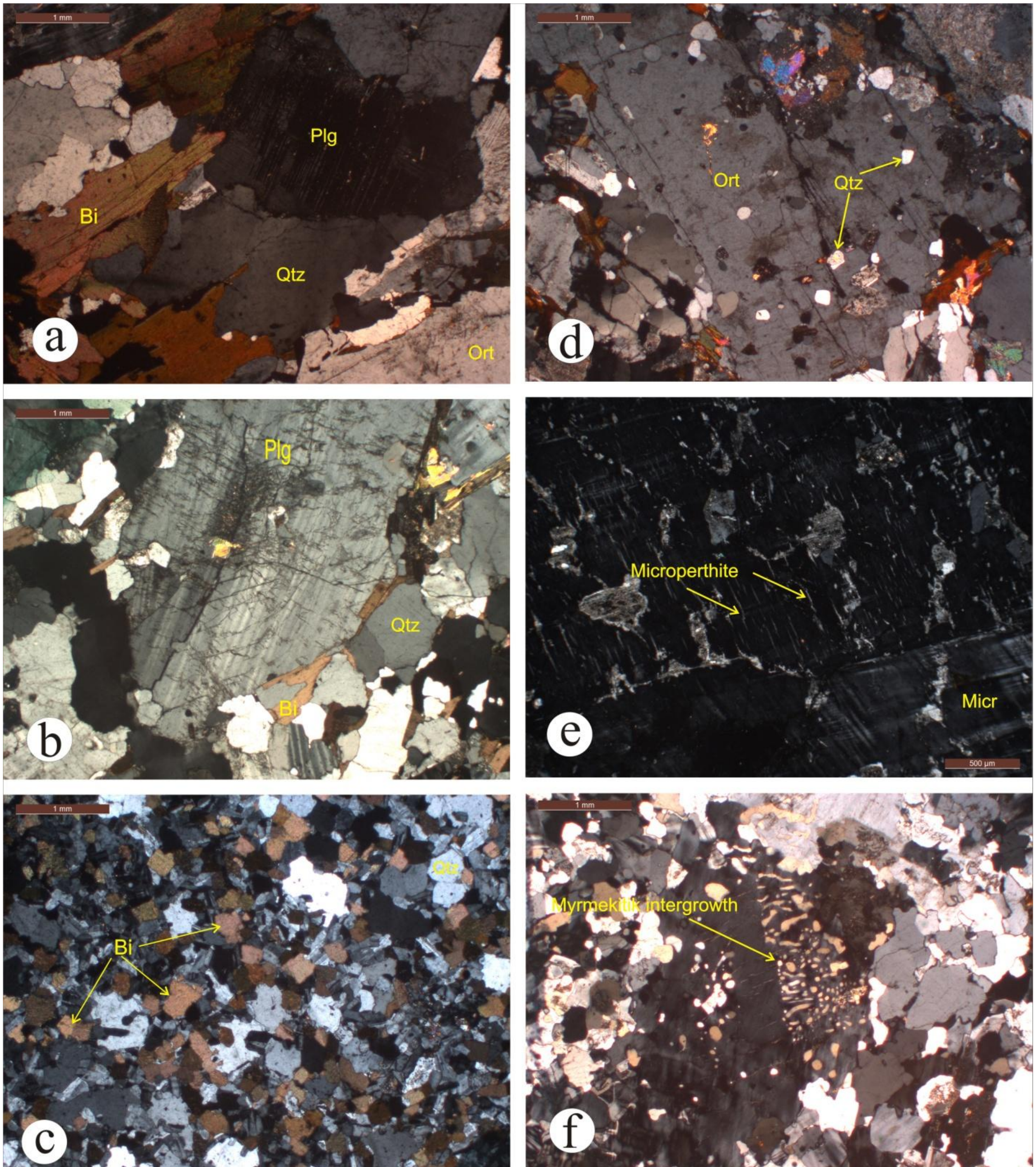

Figure 5.19: Photomicrograph of (a) coarse grained granite, loc. Mudhiyari (2.5X, CN); (b) coarse grained porphyritic granite, loc. Wadek (2.5X, CN); (c) fine grained granite, loc. Ranjitnagar (2.5X, CN); (d) granite showing poikilitic texture, orthoclase as oikocryst having presence of quartz chadacryst, loc. SE of Valothi (2.5X, CN); (e) granite showing micro-perthitic texture, loc. S of Wadek (4X, CN); (f) granite showing myrmekitic texture, loc. Dev Dungar, (2.5X, CN).

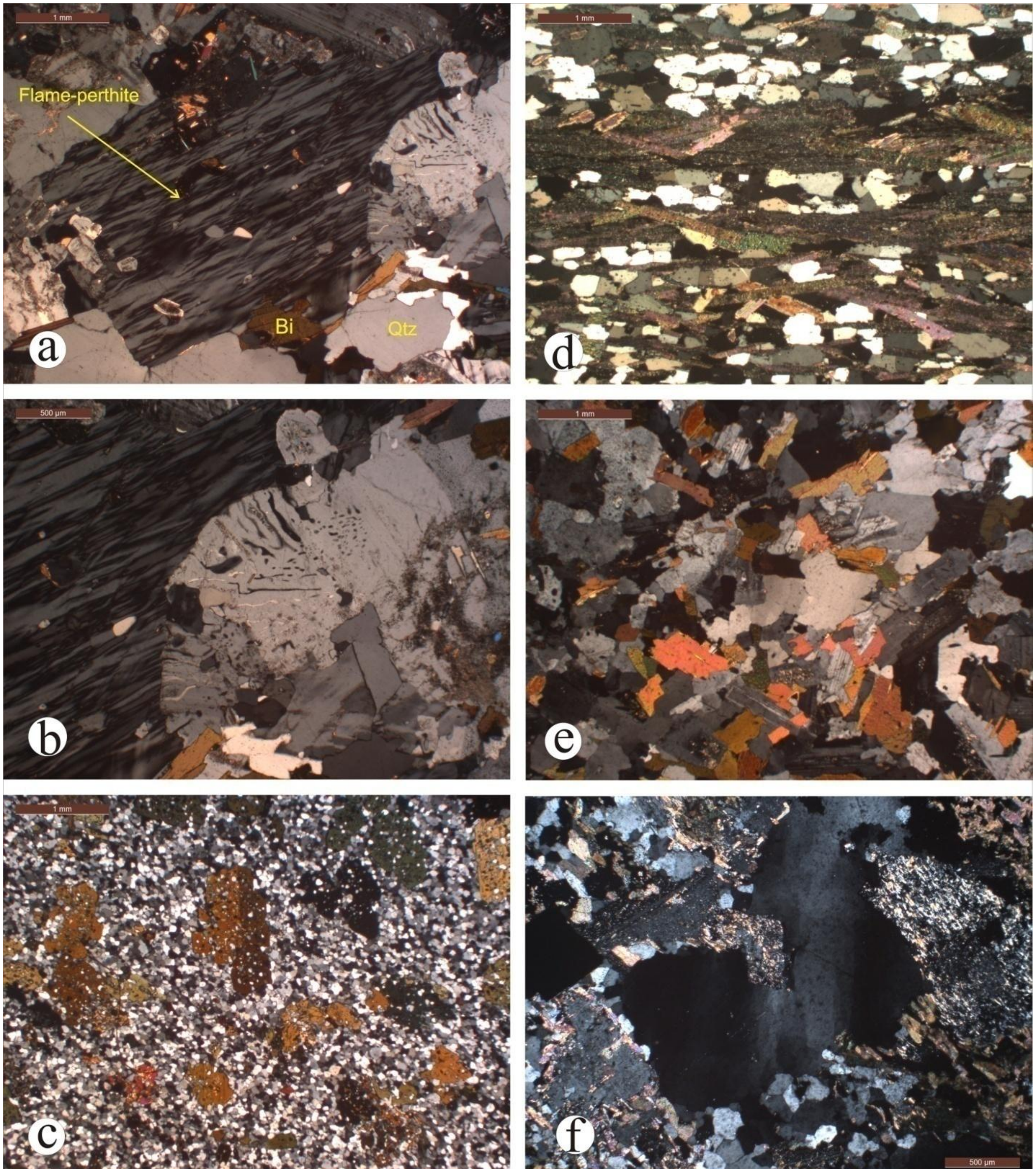

Figure 5.20: Photomicrograph of (a) granite showing flame perthite, loc. Zab village (2.5X, CN); (b) granite showing myrmekitic texture, loc. Sukhi dam, (4X, CN); (c) calc-silicate rock xenolith showing hornfelsic texture, loc.SE of Valothi (2.5X, CN); (d) xenolith of schist showing schistose texture, loc. Sukhi Dam site (2.5X, CN); (e) xenolith of fine grained granite, loc. Ranjitnagar (2.5X, CN); (f) granite having undulose quartz, loc. Nani Khatva (4X, CN).

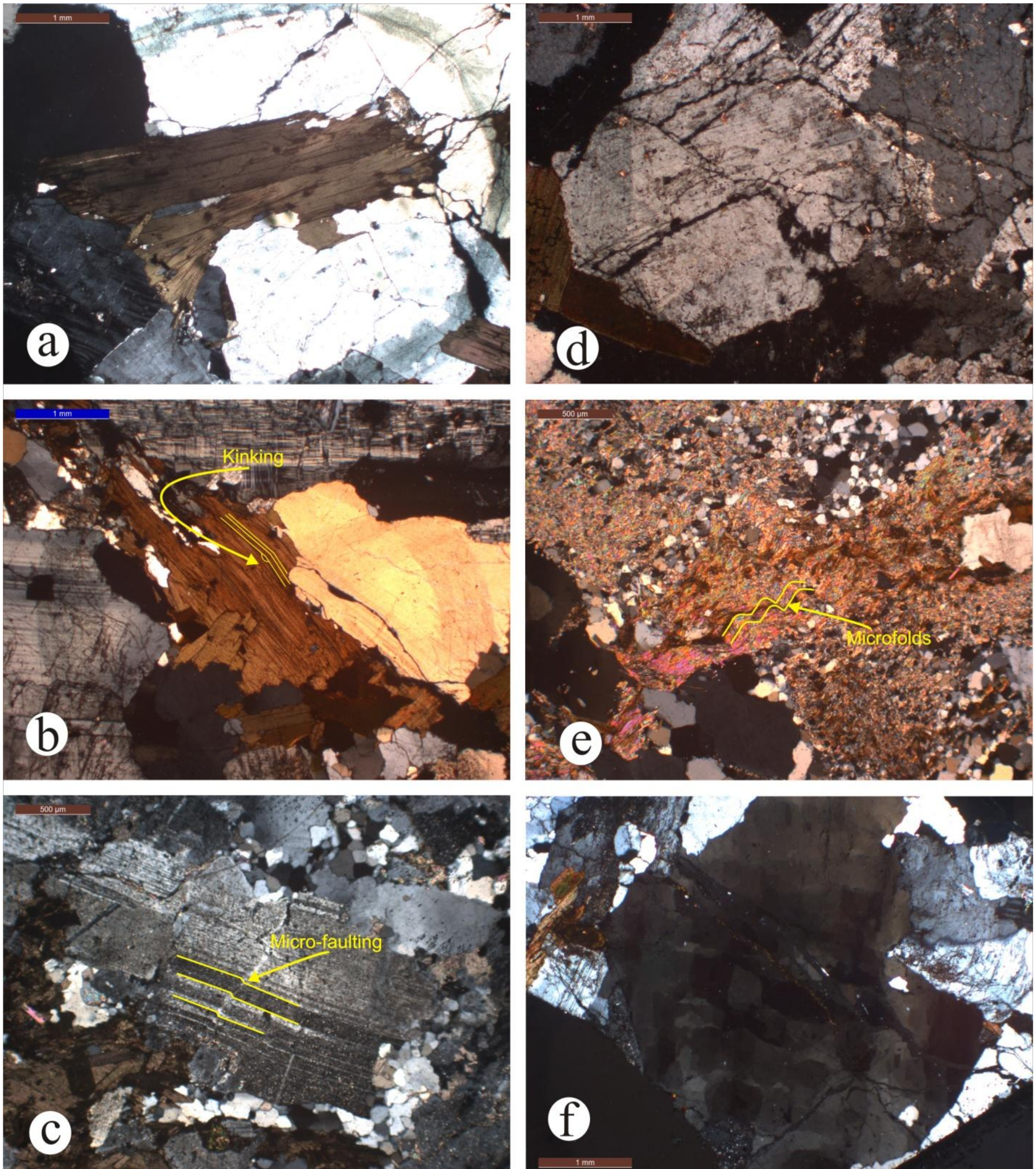

Figure 5.21: Photomicrograph of granite (a) having undulose biotite, loc. Nani Khatva (2.5X, CN); (b) having kinking in biotite, loc. Nani Khatva (2.5X, CN); (c) having micro faulting in plagioclase feldspar, loc. Kanpur (4X, CN); (d) having fractured quartz grains, loc. Wadek, (2.5X, CN); (e) having micro folds in mica minerals, loc. Lambhia (4X, CN); (f) having chess board extinction in quartz, loc. Mota Vajpur (2.5X, CN).

Zwart (1960, 1962) used the criteria of porphyroblast-matrix relationship for the first time and gave an elaborative scheme with nine diagnostic relations dependent on the idea of grain growth to be older, younger or of the similar age with respect to the deformation phases (Fig. 5.22). The said relationship of the grain growth is based on the internal schistosity planes (within the porphyroblast) as Si and external fabric or matrix orientation as Se. Further, Passchier and Trouw, (2005) added one more criteria as 'inter-tectonic' on the basis of Si-Se relationship in which the inclusion trails within the porphyroblasts have no continuity with the external fabric (Fig. 5.23). Similar studies have also been carried out by Mamtani and Karanth (1996c) to differentiate syn-tectonic from post-tectonic porphyroblasts on the basis of the extinction of inclusions. Their work suggests that the inclusion within syn-tectonic porphyroblasts possesses undulose extinction, whereas those in case of post-tectonic porphyroblasts reflect sharp extinction (Mamtani and Karanth, 1996c).

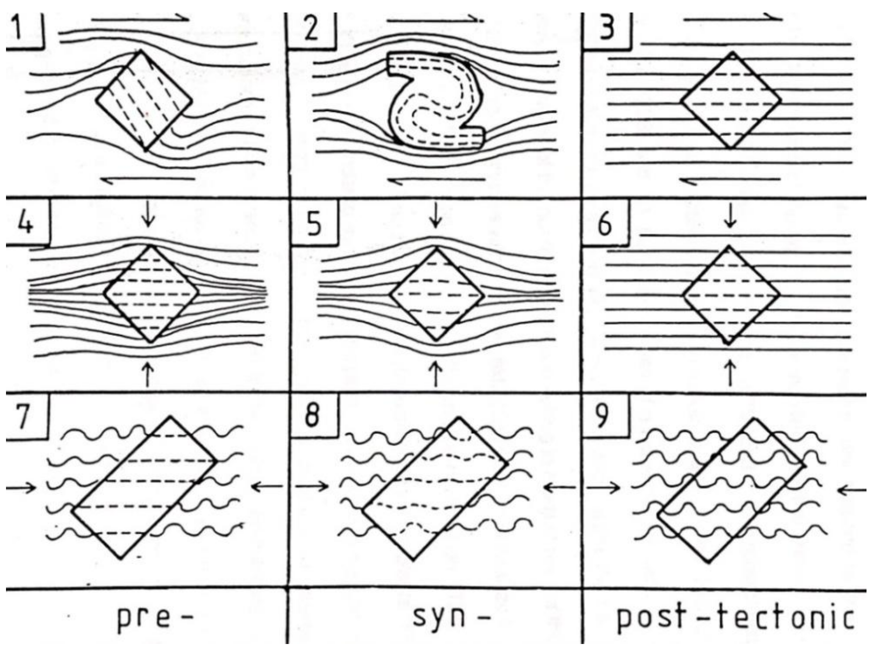

Figure 5.22: Nine diagnostic Porphyroblast-matrix relationship based on internal (Si ~ dotted lines) and external (Se ~ continuous lines) schistosity planes. (after Zwart, 1962)

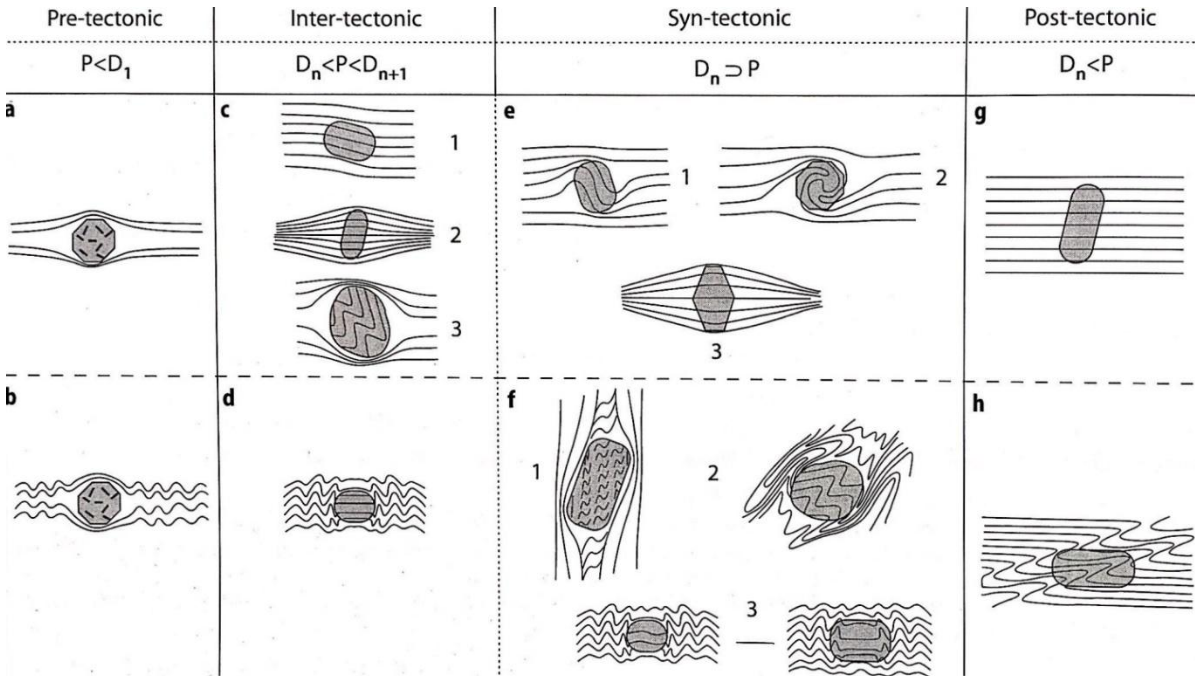

Figure 5.23: Schematic representation of pre, inter, syn and post-tectonic porphyroblast growth. The upper part of the diagram shows deformation resulting in a single foliation, while the lower part depicts deformation resulting in crenulation of an older foliation. (after, Passchier and Trouw, 2000)

As mentioned in the structural setup of the study area (Chapter 4), the Champaner Group has experienced three phases of deformation, viz. D_1, D_2 and D_3. D_1 and D_2 phases are co-axial to develop F_1 and F_2 folds on account of regional deformation along with syn-tectonic emplacement of granite. F_1 folds are of moderately inclined nature having WNW-ESE trend, whereas F_2 folds are of tight-isoclinal variety with E-W trend. Manifestation of F_2 folds over F_1 in older formations of the Champaner Group represent sub-parallel relationship with S_0-S_1 and axial planar S_2 schistosity plane has been developed generating L_2 lineations on S_0. The younger formations of the Champaner Group exhibit F_1 folds of second order tight, whereas F_2 folds show first order open with varying amplitude versus wavelength ratio. D_3 phase of deformation has generated N-S trending F_3 cross folds of open variety over kilometer long limbs of F_1 and F_2 folds. The culminating phase of the Champaner deformation is marked by post-tectonic granites, which has been responsible for the development of F_3 folds, sinistral/ dextral faults throughout the group and cross-sectional reverse shears in vicinity of the Narukot dome.

Microstructural derivatives of deformational episodes as well as signatures of prolonged emplacement of granites (from syn-to-post) have been significantly recorded within the meta-pelites of the Champaner Group. Table. 5.2 summarize the time relationship between crystallization and deformation of various minerals in metapelites of the study area. The older formations located at the eastern part of the study area inside Narukot dome and younger formations encountered along western direction near Bhat represents D_1 deformation. These rocks mainly composed of graphite schists along east and Mn-phyllites towards west, show progressive regional metamorphism M_1. Manifestation of D_2 over D_1 has given rise to M_2 metamorphism. These rocks show the presence of differentiated crenulation cleavage with three prominent surfaces (S_0, S_1 and S_2). S_1 and S_2 have developed during D_1 and D_2 respectively. Mineral development along S_0 sub-parallel to S_1 suggests chlorite + muscovite + biotite and quartz, whereas in case of S_2 minor occurrences of muscovite + biotite are seen (Figs. 5.24a-b).

Areas predominantly representing D_2 phase of deformation, NW of Narukot near Borkas represent discrete crenulation cleavage in phyllites. They have preserved primary lithological layering (S_0) which is marked by alternating layers of quartz rich and mica rich layers (Fig. 5.24c). The first schistosity fabric (S_1) sub-parallel to the bedding comprises chlorite + muscovite + biotite and quartz. The second schistosity fabric (S_2) formed on account of folding of S_1 lies at the high angles with respect to S_0 II S_1 (Fig. 5.24d). Development of minerals along S_2 suggests muscovite + biotite + garnet ± quartz. M_2 metamorphic event has been progressive from biotite to garnet grade. The garnets are found to be developed during syn-D_2 event having helicitic inclusion trails of undulose quartz (Fig. 5.25a).

D_1 and D_2 phase of deformation have also been accompanied by syn-tectonic granite emplacement. The areas along the eastern margin in vicinity of the granite at Wadek and Jharav show the development of contact metamorphic minerals such as andalusite, sillimanite and cordierite. The andalusite within the hornfelses of the Wadek region shows oppositely concave microfolds (OCMs) and is of syn-tectonic origin (Fig. 5.18a). These rocks are also characterized by the presence of sillimanite (fibrolite) along the andalusite- quartz margins (Fig. 5.25b). In case of hornfelses near Jharav, show inter-tectonic relationship of cordierite poikiloblasts in which S_0 sub-parallel S_1 fabric can be appreciated having no continuity with the inclusion trails present inside the host (Fig. 5.25c). During D_3 phase of deformation no mineral development cutting across D_1 and D_2 have been evident, hence it can be inferred that D_3 phase of deformation was devoid of any metamorphism.

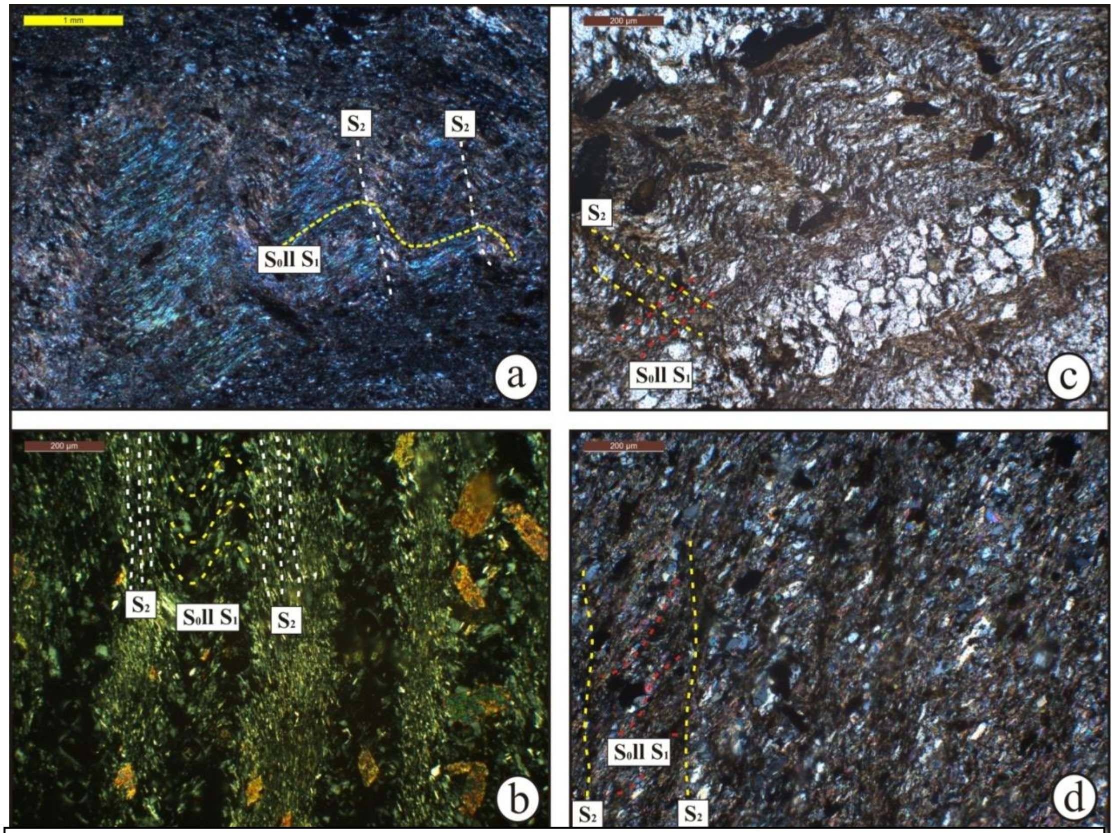

Figure 5.24: Photomicrograph of (a) graphite schist from Narukot dome (2.5XCN) showing differentiated crenulations cleavage. S_2 is at high angle with respect to S_0 sub parallel S_1; (b) Mn-rich phyllites from Bhat (10XCN) showing continuous crenulation cleavage. S_0 ll S_1 is found to be folded to generate S_2 schistosity fabric; (c) phyllite near Borkas (10XPPL) showing discrete crenulation cleavage. The bedding plane S_0 is defined by the contact between quartz rich and quartz poor layers. The S_2 has developed along phyllosilicate rich layers at high angles to S_0 ll S_1; (d) phyllite located north of Malabar (10XCN) depicting discontinuous crenulation cleavage. S_0 is sub parallel to S_1 is folded to develop S_2.

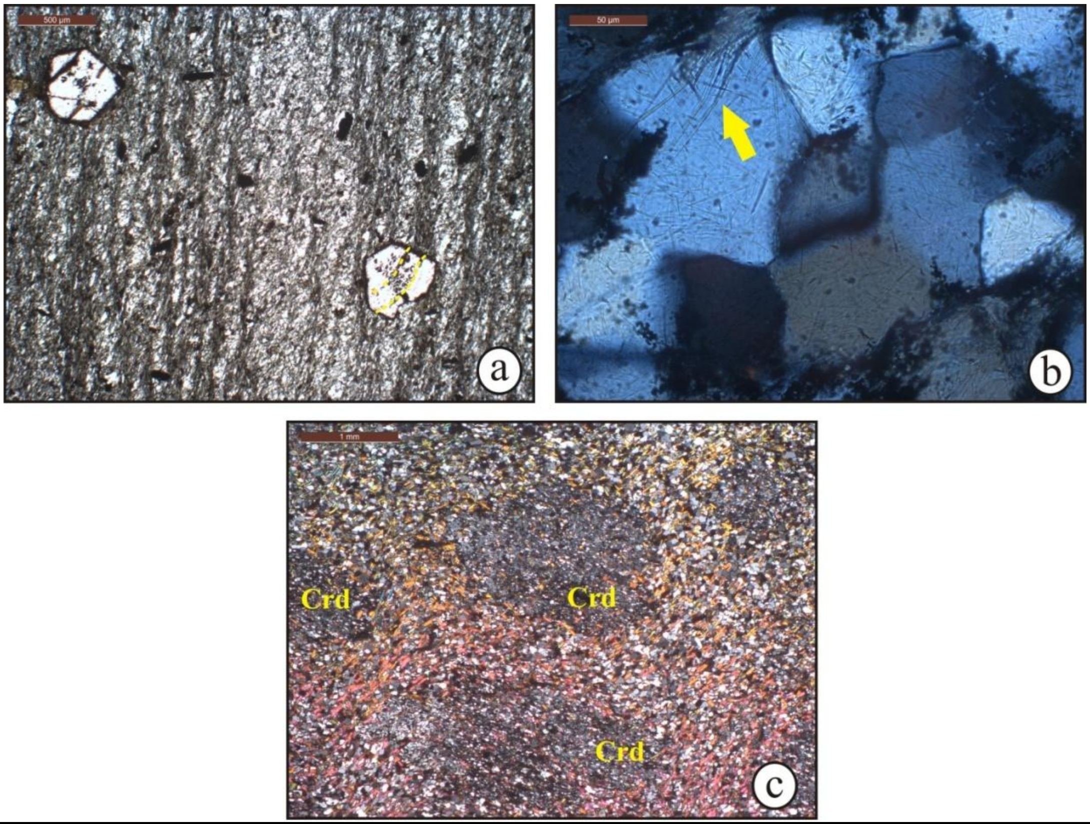

Figure 5.25: Photomicrograph of (a) phyllite located north of Malabar (4XPPL) showing syn-D_2 garnets. The euhedral granets possess spiral inclusion trails of quartz; (b) andalusite hornfels from Wadek (40XCN) showing development of sillimanite (fibrolite) along andalusite quartz margins; (c) cordierite hornfels (2.5XCN) showing unmatched internal fabric (S_i) with external schistosity plane (S_e).

Lastly, the D3 deformation event of the Champaner Group marked by post-tectonic granites has caused metasomatic introductions of mineral phases in the country rocks. These metasomatic effects are evident by the occurrences of muscovite over andalusite in hornfelses and tourmaline within the quartzites located nearer to the granite due to alkali and boron rich metasomatism respectively.

Mineral development during regional metamorphism	Corelatable Deformational Events		
	D1	***D2***	***D3***
Chlorite 1	------		
Chlorite 2		------	
Muscovite 1	------	------	
Biotite 1	------		
Biotite 2		------	
Garnet		------	
Quartz	------	------	

Mineral development during contact metamorphism	Prolong Magmatic Event	
	Syn-tectonic granites	**Post-tectonic granites**
Andalusite	---------------	
Cordierite	---------------	
Sillimanite (Fibrolite)	---------------	
Muscovite 2		------
Tourmaline		------

Table 5.2: Time relationship between crystallization and deformation of various minerals in meta-pelites of the study area. The former part of the table indicates the mineral development due to regional metamorphism, where as the later enumerates the grain growth due to syn-to-post granite emplacement.

----------*END*----------